J|A|C|S
ARTICLES
Published on Web 04/22/2004

3,5-Pyridyne—A Heterocyclic *meta*-Benzyne Derivative

Michael Winkler, Bayram Cakir, and Wolfram Sander*

Contribution from the Lehrstuhl für Organische Chemie II der Ruhr-Universität Bochum, Universitätsstrasse 150, 44780 Bochum, Germany

Received October 21, 2003; E-mail: Wolfram.Sander@rub.de

Abstract: 3,5-Pyridyne (**3**) has been generated by flash vacuum pyrolysis of 3,5-diiodopyridine (**20**) and 3,5-dinitropyridine (**21**) and characterized by IR spectroscopy in cryogenic argon matrices. The aryne can clearly be distinguished from other side products by its photolability at 254 nm, inducing a rapid ring-opening presumably to (*Z*)-1-aza-hex-3-ene-1,5-diyne. As byproducts of the pyrolysis, HCN and butadiyne were identified, together with traces of acetylene, cyanoacetylene, (*E*)-1-aza-hex-3-ene-1,5-diyne, and the 3-iodo-5-pyridyl radical (from **20**). Several pathways for rearrangements and fragmentations of **3** and of the parent *meta*-benzyne (**1**) have been explored computationally by density functional theory and ab initio quantum chemical methods. The lowest energy decomposition pathway of biradicals **1** and **3** is a ring-opening process accompanied by hydrogen migration, leading to (*Z*)-hex-3-ene-1,5-diyne [(*Z*)-**10**] and (*Z*)-3-aza-hex-3-ene-1,5-diyne [(*Z*)-**24**], respectively. Both reactions require activation energies of 45−50 kcal mol^{-1}. Mechanisms leading from (*Z*)-**24** or directly from **3** to the experimentally observed byproducts are discussed. Upon replacement of the C(5)H moiety by N in *meta*-benzyne, high-level calculations predict a modest shortening of the interradical distance by 5−7 pm and a reduction of the singlet−triplet energy splitting by 3 kcal mol^{-1}, in good agreement with isodesmic equations, according to which the singlet ground state of **3** is destabilized relative to **1** by 3−4 kcal mol^{-1}. In contrast to 3,5-borabenzyne (**2**), which is found to be doubly aromatic, nucleus-independent chemical shifts of **3** are almost identical to that of pyridine, indicating the absence of paramagnetic ring current effects that may be associated with "in-plane antiaromaticity". As compared with **1**, the overall perturbation caused by the nitrogen atom in **3** is weak, and four electron, three center interaction is of minor importance in this molecule.

Introduction

Arynes[1] are useful reactive intermediates in synthesis,[2] and they also play a crucial role in a number of important processes, among them the biological activity of cytostatics,[3] combustion reactions,[4] and heterogeneous catalysis.[5] Interest in heterocyclic arynes[6] increased recently due to their potential application as more selective warheads in endiyne antitumor agents.[7−9] Accordingly, the structure and reactivity of nitrogen-containing 1,4-arynes and their corresponding enediyne precursors have been investigated in some detail.[7−13] Heterocyclic *meta*-benzyne derivatives, on the other hand, have not yet received the attention they deserve, and up to now, even the chemistry of the parent *meta*-benzyne (**1**) is not completely understood, especially with regard to its reactivity toward electrophiles, nucleophiles, and radicals.[14]

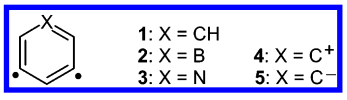

The structure of *meta*-benzyne has been clarified recently; on the basis of high-level calculations, it has been shown that **1** adopts a monocyclic structure in which the distance of the

(1) (a) Wenk, H. H.; Winkler, M.; Sander, W. *Angew. Chem.* **2003**, *115*, 518; *Angew. Chem., Int. Ed.* **2003**, *42*, 502. (b) Sander, W. *Acc. Chem. Res.* **1999**, *32*, 669. (c) Hoffman, R. W. *Dehydrobenzene and Cycloalkynes*; Academic Press: New York, 1967.
(2) For example, see (a) Pellissier, H.; Santelli, M. *Tetrahedron* **2003**, *59*, 701. (b) Grundmann, C. In *Houben-Weyl Methoden der Organischen Chemie*; Grundmann, C., Ed.; Thieme: Stuttgart, 1981; Vol. 5.
(3) See, for example, (a) Thorson, J. S.; Sievers, E. L.; Ahlert, J.; Shepard, E.; Whitwam, R. E.; Onwueme, K. C.; Ruppen, M. *Curr. Pharm. Des.* **2000**, *6*, 1841 and references therein. (b) *Endiyne Antibiotics as Antitumor Agents*; Borders, D. B., Doyle, T. W., Eds.; Marcel Dekker: New York, 1995. (c) Nicolaou, K. C.; Smith, A. L. *Acc. Chem. Res.* **1992**, *25*, 497. (d) Nicolaou, K. C.; Dai, W.-M. *Angew. Chem.* **1991**, *103*, 1453; *Angew. Chem., Int. Ed. Engl.* **1991**, *30*, 1387.
(4) (a) Wang, H.; Laskin, A.; Moriarty, N. W.; Frenklach, M. *Proc. Combust. Inst.* **2000**, *28*, 1545. (b) Moskaleva, L. V.; Madden, L. K.; Lin, M. C. *Phys. Chem. Chem. Phys.* **1999**, *1*, 3967. (c) Madden, L. K.; Moskaleva, L. V.; Kristyan, S.; Lin, M. C. *J. Phys. Chem.* **1997**, *101*, 6790.
(5) (a) Yamagishi, S.; Jenkins, S. J.; King, D. A. *J. Chem. Phys.* **2002**, *117*, 819. (b) Johnson, K.; Sauerhammer, B.; Titmuss, S.; King, D. A. *J. Chem. Phys.* **2001**, *114*, 9539 and literature cited therein.
(6) For general reviews on heterocyclic arynes, see (a) Reinecke, M. G. *Tetrahedron* **1982**, *38*, 427. (b) Kaufmann, T.; Wirthwein, R. *Angew. Chem.* **1971**, *83*, 21; *Angew. Chem., Int. Ed. Engl.* **1971**, *10*, 20.
(7) (a) Hoffner, J.; Schottelius, M. J.; Feichtinger, D.; Chen, P. *J. Am. Chem. Soc.* **1998**, *120*, 376. See also (b) Chen, P. *Angew. Chem.* **1996**, *108*, 1584; *Angew. Chem., Int. Ed. Engl.* **1996**, *35*, 1478.
(8) Cramer, C. J. *J. Am. Chem. Soc.* **1998**, *120*, 6261.
(9) (a) Kraka, E.; Cremer, D. *J. Comput. Chem.* **2001**, *22*, 216. (b) Kraka, E.; Cremer, D. *J. Am. Chem. Soc.* **2000**, *122*, 8245. (c) Kraka, E.; Cremer, D. *J. Mol. Struct. (THEOCHEM)* **2000**, *506*, 191.
(10) (a) Feng, L.; Kerwin, S. M. *Tetrahedron Lett.* **2003**, *44*, 3463. (b) Feng, L.; Kumar, D.; Kerwin, S. M. *J. Org. Chem.* **2003**, *68*, 2234. (c) Nadipuram, A. K.; David, W. M.; Kumar, D.; Kerwin, S. M. *Org. Lett.* **2002**, *4*, 4543. (d) David, W. M.; Kerwin, S. M. *J. Am. Chem. Soc.* **1997**, *119*, 1464.
(11) (a) Debbert, S. L.; Cramer, C. J. *Int. J. Mass Spectrom.* **2000**, *201*, 1. (b) Cramer, C. J.; Debbert, S. *Chem. Phys. Lett.* **1998**, *287*, 320. For an earlier computational study of pyridynes, see (c) Nam, H. H.; Leroi, G. E.; Harrison, J. F. *J. Phys. Chem.* **1991**, *95*, 6514. See also Adam, W.; Grimison, A.; Hoffmann, R. *J. Am. Chem. Soc.* **1969**, *91*, 2590.
(12) Cioslowski, J.; Szarecka, A.; Moncrieff, D. *Mol. Phys.* **2003**, *101*, 839.
(13) Halter, R. J.; Fimmen, R. L.; McMahon, R. J.; Peebles, S. A.; Kuczkowski, R. L.; Stanton, J. F. *J. Am. Chem. Soc.* **2001**, *123*, 12353.

Scheme 1

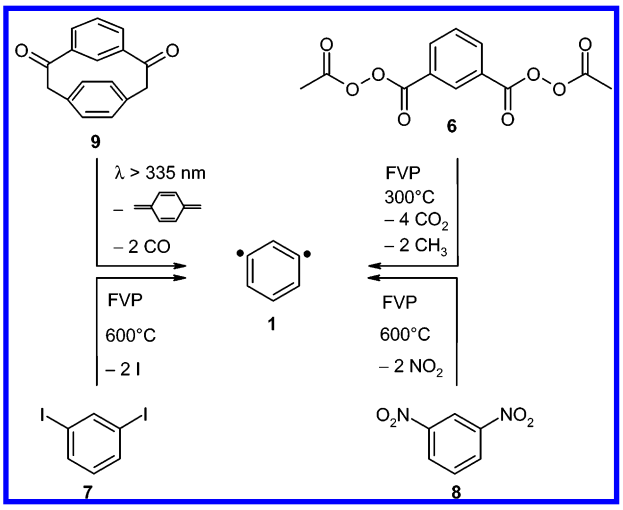

radical centers is around 205 pm, while a bicyclic *anti*-Bredt form **1b** does not occupy a stationary point on the C_6H_4 potential energy surface, which, nonetheless, is extremely flat in the region between both structures.[15] Several computational methods that work well in other cases fail in this respect and overestimate bonding between the radical sites.[16]

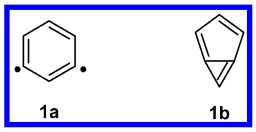

The computational predictions have been firmly established by comparison of the calculated and measured IR spectra.[17,18] The latter have been obtained in cryogenic argon matrices, where **1** was generated from four different precursors, both under flash vacuum pyrolysis (FVP) conditions (from **6** to **8**) and photochemically (from **9**) in situ (Scheme 1).[18]

In accord with earlier investigations,[19] the enediynes (*Z*)-**10** and (*E*)-**10** are formed as side products during pyrolysis of **7** and **8** at temperatures above 500 °C, and the ratio of **10**:**1** increases with temperature, suggesting a rearrangement **1** → **10** that requires a change of the CH connectivity.[20] Several pathways for this reaction have been discussed in the literature. Investigations by Zewail et al. using femtosecond time-resolved spectroscopy with mass spectrometric detection on the photolysis of 1,2-, 1,3-, and 1,4-dibromobenzene have been interpreted by

Scheme 2

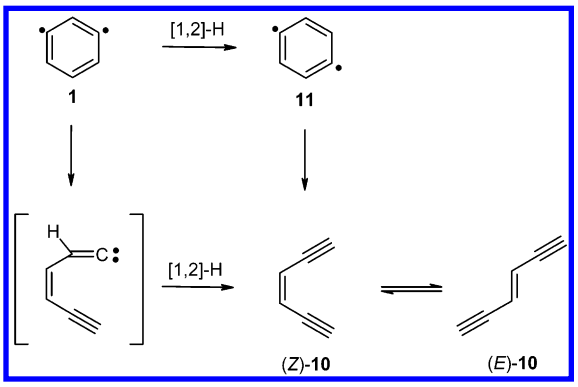

the authors in terms of a rapid equilibrium between *ortho*-, *meta*-, and *para*-benzyne via quantum mechanical tunneling of H atoms, from which the *para*-isomer **11** reacts to the entropically favored enediyne **10**.[21] According to B3LYP/6-31G** calculations, however, a different mechanism, in which ring-opening of **1** and hydrogen migration proceed in one step, appears to be more likely (Scheme 2).[18,22]

Aza-analogues of the benzynes have been studied computationally by Cramer and Debbert,[11] Ciosloswski et al.,[12] and Kraka and Cremer.[9] Similar to **1**, the calculated equilibrium structures (monocyclic vs bicyclic) of the *meta*-pyridynes show a pronounced dependence on the level of theory employed. The electronic effects of the nitrogen lone pair have been interpreted in terms of a σ-allylic four electron, three center interaction, which destabilizes the singlet ground states of 3,5-pyridyne (**3**) and in particular that of 2,6-pyridyne (**12**), the lowest singlet and triplet states of which are almost degenerate. In contrast, the 2,4-isomer **13** is slightly stabilized relative to **1** [based on calculated biradical stabilization energies (BSE), vide infra] by virtue of strong contributions of a nitrilium ion structure to the resonance hybrid.[11] Compounds **12**, **3**, and **13** are less stable than the lowest energy 3,4-pyridyne (**14**) by 17.5, 14.7, and 1.2 kcal mol^{-1}, respectively [CAS(8,8)PT2/cc-pVDZ//CAS(8,8)-SCF/cc-pVDZ].[11]

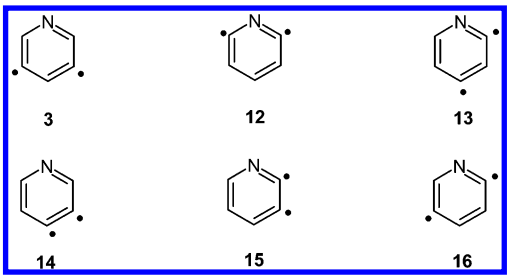

In contrast to the four electron, three center interaction, a two electron, three center system in the plane of the aromatic ring is strongly stabilizing, e.g., in the 3,5-didehydrophenyl cation (**4**) (D_{3h}), the classic example[23] of "in-plane aromaticity",

(14) For interesting studies on the reactivity of charged *meta*-benzyne derivatives employing the distonic ion approach, see (a) Price, J. M.; Nizzi, K. E.; Campbell, J. L.; Kenttämaa, H. I.; Seierstad, M.; Cramer, C. J. *J. Am. Chem. Soc.* **2003**, *125*, 131. (b) Nelson, E. D.; Artau, A.; Price, J. M.; Tichy, S. E.; Jing, L.; Kenttämaa, H. I. *J. Phys. Chem. A* **2001**, *105*, 10155. (c) Nelson, E. D.; Artau, A.; Price, J. M.; Kenttämaa, H. I. *J. Am. Chem. Soc.* **2000**, *122*, 8781. (d) Thoen, K. K.; Kenttämaa, H. I. *J. Am. Chem. Soc.* **1999**, *121*, 800.

(15) (a) Winkler, M.; Sander, W. *J. Phys. Chem. A* **2001**, *105*, 10422. (b) Kraka, E.; Anglada, J.; Hjerpe, A.; Filatov, M.; Cremer, D. *Chem. Phys. Lett.* **2001**, *348*, 115.

(16) (a) Hess, B. A., Jr. *Eur. J. Org. Chem.* **2001**, 2185. See refs 15 and 18 for a correction of the conclusions drawn in that work. The related but formally symmetry-forbidden cyclization of *para*-benzyne to butalene has been investigated using density functional theory and coupled cluster methods. (b) Warner, P. M.; Jones, G. B. *J. Am. Chem. Soc.* **2001**, *123*, 10322 and ref 15b.

(17) Marquardt, R.; Sander, W.; Kraka, E. *Angew. Chem.* **1996**, *108*, 825; *Angew. Chem., Int. Ed. Engl.* **1996**, *35*, 746.

(18) Sander, W.; Exner, M.; Winkler, M.; Balster, A.; Hjerpe, A.; Kraka, E.; Cremer, D. *J. Am. Chem. Soc.* **2002**, *124*, 13072.

(19) Fisher, I. P.; Lossing, F. P. *J. Am. Chem. Soc.* **1963**, *85*, 1018.

(20) Sander, W.; Marquardt, R.; Bucher, G.; Wandel, H. *Pure Appl. Chem.* **1996**, *68*, 353.

(21) Diau, E. W.-G.; Casanova, J.; Roberts, J. D.; Zewail, A. H. *Proc. Natl. Acad. Sci. U.S.A.* **2000**, *97*, 1376.

(22) The formation of vinylidene intermediates from various *meta*-benzyne derivatives has been proposed by Brown et al., e.g., (a) Brown, R. F. C. *Eur. J. Org. Chem.* **1999**, *3211*, 1 and references therein. (b) Brown, R. F. C.; Eastwood, F. W. *Pure Appl. Chem.* **1996**, *68*, 261. For a rearrangement of 1,3-didehydronaphthalene to diethynylbenzene under high-temperature conditiones, see (c) Grützmacher, H.-F.; Lohmann, J. *Liebigs Ann. Chem.* **1975**, 2023.

(23) Chandrasekhar, J.; Jemmis, E. D.; Schleyer, P. v. R. *Tetrahedron Lett.* **1979**, 3707.

and the global minimum on the $C_6H_3^+$ potential energy surface.[24] This interesting system has recently been detected for the first time in a FT-ICR mass spectrometer by Kentämaa et al.[25] The corresponding anion **5**, which is isoelectronic to **3**, has been characterized in the gas phase by Hu and Squires.[26] The observed reactivity of **5** is in agreement with a ground state singlet anion with a Jahn−Teller distorted C_{2v} structure (see, however, ref 27). It has been argued that **5** may be considered to be the antiaromatic analogue of **4**, but a justification for that notion (e.g., based on energetic or magnetic aromaticity criteria) is not available yet.[26,28] More recently, Wenthold et al. determined the heat of formation of 1,3,5-tridehydrobenzene (**17**) ($^2A_1$), which takes an intermediate position between **4** and **5**.[28] The first and third bond dissociation energies (BDE) of benzene (**18**) are very similar while the second is considerably lower; therefore, **17** is best described as a phenyl radical that interacts only weakly with a *meta*-benzyne moiety on the opposite side of the ring.[28]

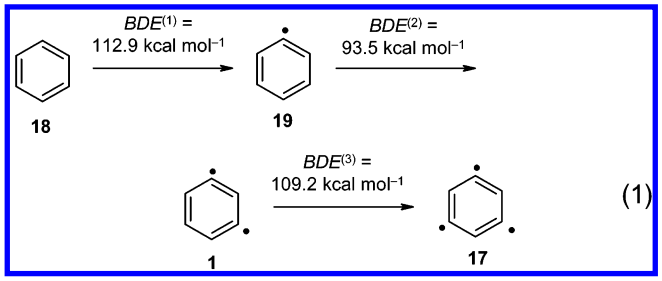

Despite the fundamental interest in pyridynes and related or isoelectronic systems, direct spectroscopic information on these molecules is scarce. The only hetaryne that has so far been characterized by IR spectroscopy is 3,4-pyridyne (**14**).[29] In this contribution, we describe the matrix isolation and IR spectroscopic characterization of 3,5-pyridyne (**3**). The article is arranged as follows: First, we discuss the FVP experiments of 3,5-diiodopyridine (**20**) and 3,5-dinitropyridine (**21**). The measured IR spectrum of **3** is subsequently compared with calculated vibrational spectra, and complemented by high-level ab initio calculations, the structure of 3,5-pyridyne is elucidated. The next part is devoted to the electronic structure of **3** [and comparison with 3,5-borabenzyne (**2**)], and the notation of in-plane aromaticity/antiaromaticity is evaluated critically on the basis of energetic and magnetic arguments. Finally, we discuss the kinetic stability and intramolecular rearrangements of the title compound and compare the calculated data to the experimental findings.

Results and Discussion

Matrix Isolation of 3,5-Pyridyne. In analogy to our previous matrix isolation study of *meta*-benzyne,[18] we carried out FVP of diiodopyridine **20** at temperatures around 600 °C in the gas phase with subsequent trapping of the thermolysis products in a large excess of argon at 10 K. The IR spectrum of a matrix containing the FVP products of **20** is shown in Figure 1. Apart from some unreacted starting material and the usual impurities (H_2O, CO, and CO_2) that are always found in FVP experiments, several new absorptions are detected in the ≡C−H stretching region around 3300 cm^{-1}, indicating the formation of ring-opened, acetylenic byproducts. Another prominent band is observed at 560.5 cm^{-1}. This IR band and several other, less intense signals below 2000 cm^{-1} rapidly decrease upon short wavelength (254 nm) irradiation. From the decay kinetics of these bands during photolysis, at least two distinct species can be deduced. Simultaneously, a new acetylenic compound is formed that is not present (or only in very small amounts) in the original matrix after trapping the FVP products of **20**.

Strong absorptions around 550 cm^{-1} are a characteristic feature in the vibrational spectra of **1** and derivatives substituted in the 5-position.[17,18,30] By comparison with IR spectra calculated at the BLYP level of theory, the photolabile species are readily identified as the 3-iodo-5-pyridyl radical (**22**) and 3,5-pyridyne (**3**) (Figure 2).

To further establish these assignments, we also investigated the FVP of 3,5-dinitropyridine (**21**). The same photolabile absorptions assigned to **3** can also be identified in the vibrational spectrum of the FVP products of **21** (Figure 3 and Table 1), while those associated with **22** are absent, confirming the conclusions drawn above.

Structural assignments of the photostable acetylenic byproducts formed thermally from **20**/**21** or photochemically from **3** are more challenging. Reasonable candidates involve several C_5H_3N isomers, e.g., **23**−**25**, or fragmentation products such as diacetylene (**26**) and cyanoacetylene (**27**).

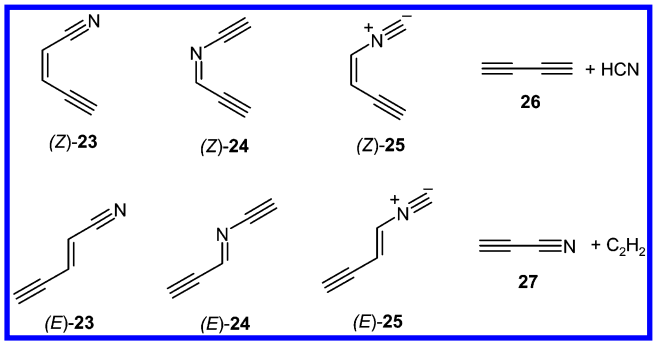

By comparison with authentic samples and reference data, we can unambiguously identify significant amounts of HCN (721.0 and 3306.5 cm^{-1})[31] and **26** (627.5 and 3326.5 cm^{-1})[32] as well as traces of acetylene (737.0, 3289.0, and 3303.0 cm^{-1})[32] and cyanoacetylene (667.5 and 3316.0 cm^{-1})[33] among the FVP products. Another characteristic signal at 947.0 cm^{-1} can be

(24) Schleyer, P. v. R.; Jiao, H.; Glukhovtsev, M. N.; Chandrasekhar, J.; Kraka, E. *J. Am. Chem. Soc.* **1994**, *116*, 10129.
(25) Nelson, E. D.; Kenttämaa, H. I. *J. Am. Soc. Mass Spectrom.* **2001**, *12*, 258.
(26) Hu, J.; Squires, R. R. *J. Am. Chem. Soc.* **1996**, *118*, 5816.
(27) Slipchenko, L. V.; Krylov, A. I. *J. Chem. Phys.* **2003**, *118*, 9614.
(28) (a) Lardin, H. A.; Nash, J. J.; Wenthold, P. G. *J. Am. Chem. Soc.* **2002**, *124*, 12612. For computational investigations of **17**, see (b) Bettinger, H. F.; Schleyer, P. v. R.; Schaefer, H. F., III. *J. Am. Chem. Soc.* **1999**, *121*, 2829 and ref 27.
(29) (a) Nam, H.-H.; Leroi, G. E. *J. Am. Chem. Soc.* **1988**, *110*, 4096. Related attempts to generate and characterize the 2,3-isomer (**15**) by photolysis of 2,3-pyridinedicarboxylic anhydride in cryogenic nitrogen matrices were unsuccessful. (b) Nam, H. H.; Leroi, G. E. *Tetrahedron Lett.* **1990**, *31*, 4837. (c) Dunkin, I. R.; MacDonald, J. G. *Tetrahedron Lett.* **1982**, *23*, 4839. See also (d) Cava, M. P.; Mitchell, M. J.; DeJongh, D. C.; Van Fossen, R. Y. *Tetrahedron Lett.* **1966**, *26*, 2947. (e) August, J.; Kroto, H. W.; McNaughton, D.; Phillips, K.; Walton, D. R. M. *J. Mol. Spectrosc.* **1988**, *130*, 424.
(30) Sander, W.; Exner, M. *J. Chem. Soc., Perkin Trans. 2* **1999**, 2285.
(31) Abbate, A. D.; Moore, C. B. *J. Chem. Phys.* **1985**, *82*, 1255.
(32) (a) Wrobel, R. Ph.D. Thesis, Ruhr-Universität Bochum, 1998. (b) Gantenberg, M. Ph.D. Thesis, Ruhr-Universität Bochum, manuscript in preparation. (c) Marquardt, R.; Sander, W. Unpublished results.
(33) Guennoun, Z.; Couturier-Tamburelli, I.; Pietry, N.; Aycard, J. P. *Chem. Phys. Lett.* **2003**, *368*, 574.

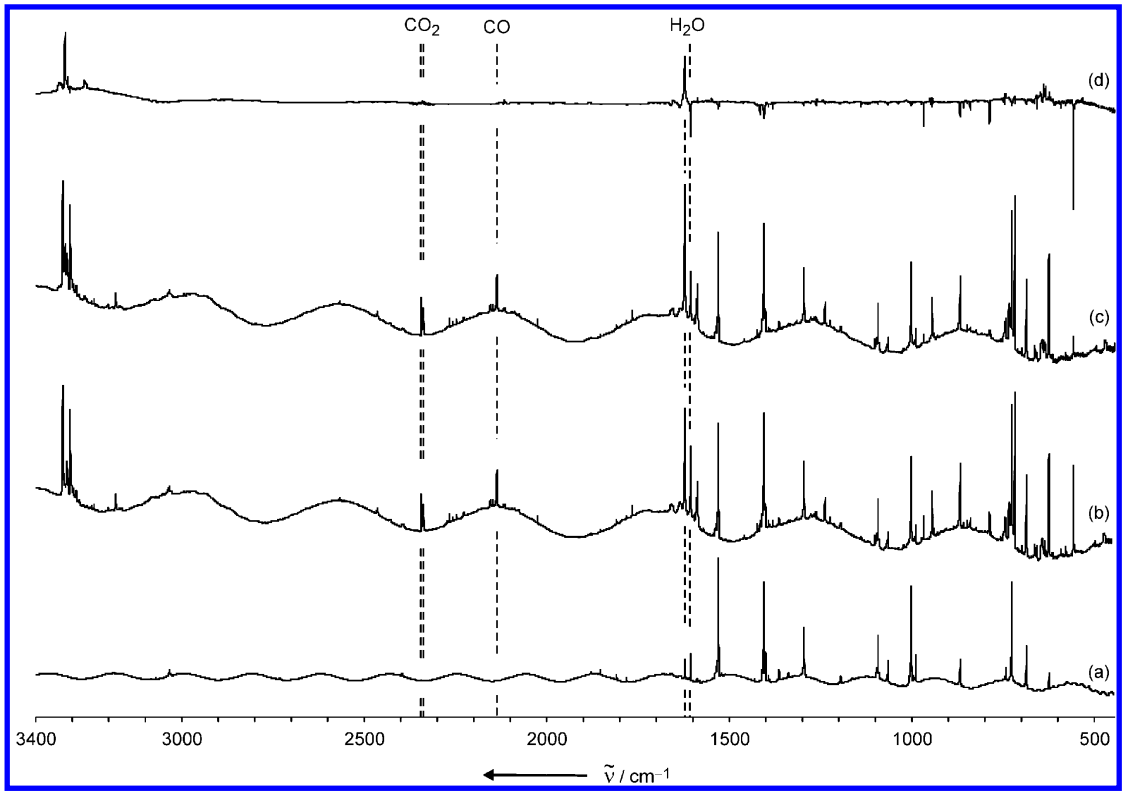

Figure 1. (a) IR spectrum of 3,5-diiodopyridine (**20**) (Ar, 10 K). (b) IR spectrum of a matrix containing the FVP products of **20**. (c) Spectrum of the same matrix after irradiation with $\lambda = 254$ nm. (d) Difference spectrum c − b; bands pointing downward decrease in intensity upon irradiation of a matrix containing the FVP products of **20**.

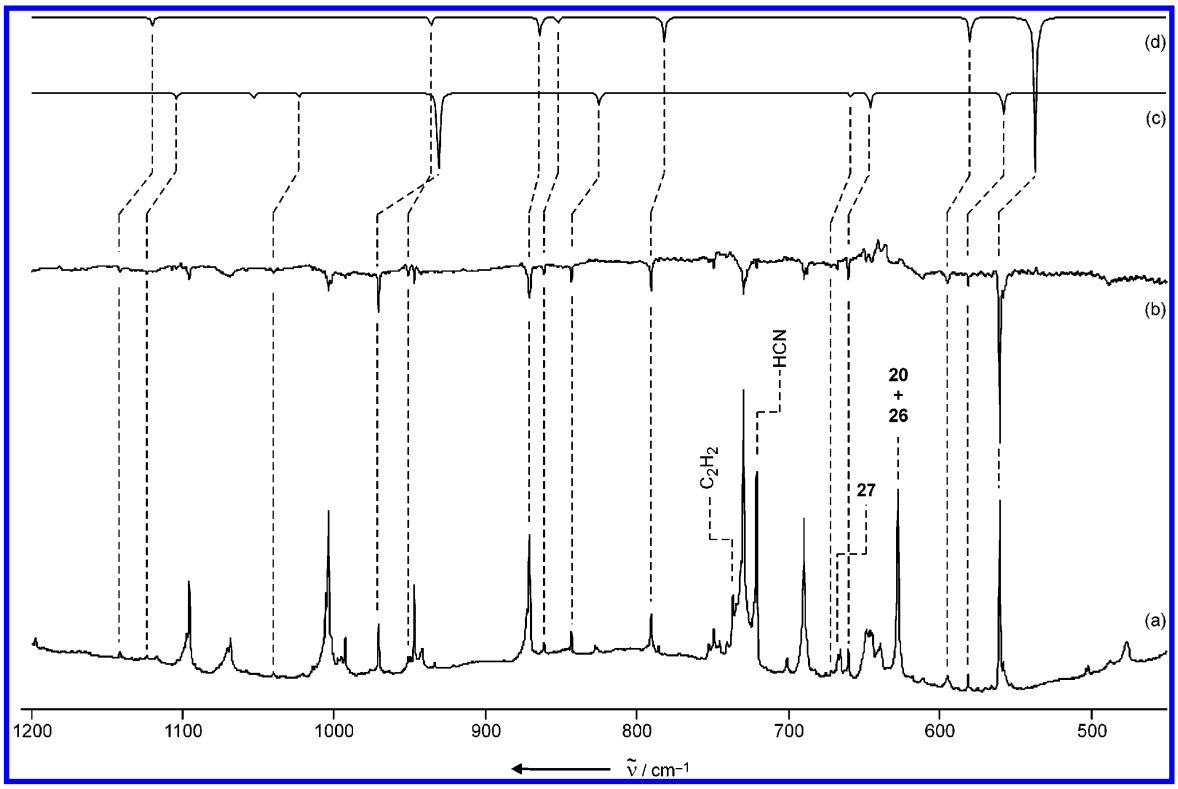

Figure 2. Comparison of measured and calculated vibrational spectra. (a) IR spectrum of a matrix containing the FVP products of **20**. (b) Difference spectrum; bands pointing downward decrease in intensity upon irradiation ($\lambda = 254$ nm) of a matrix containing the FVP products of **20**. (c) Calculated IR spectrum of 3-iodo-5-pyridyl (**22**) (UBLYP/6-311G**). (d) Calculated IR spectrum of 3,5-pyridyne (**3**) (BLYP/cc-pVTZ).

assigned to (*E*)-**23**, although it should be noted that the vibrational spectra of **23**−**25** simulated at the density functional theory (DFT) level are too similar to allow a rigorous differentiation between isomers on the basis of calculations alone (cf., Figure 1S). However, formation of (*E*)-**23** (the global minimum on the C_5H_3N potential energy surface, vide infra)

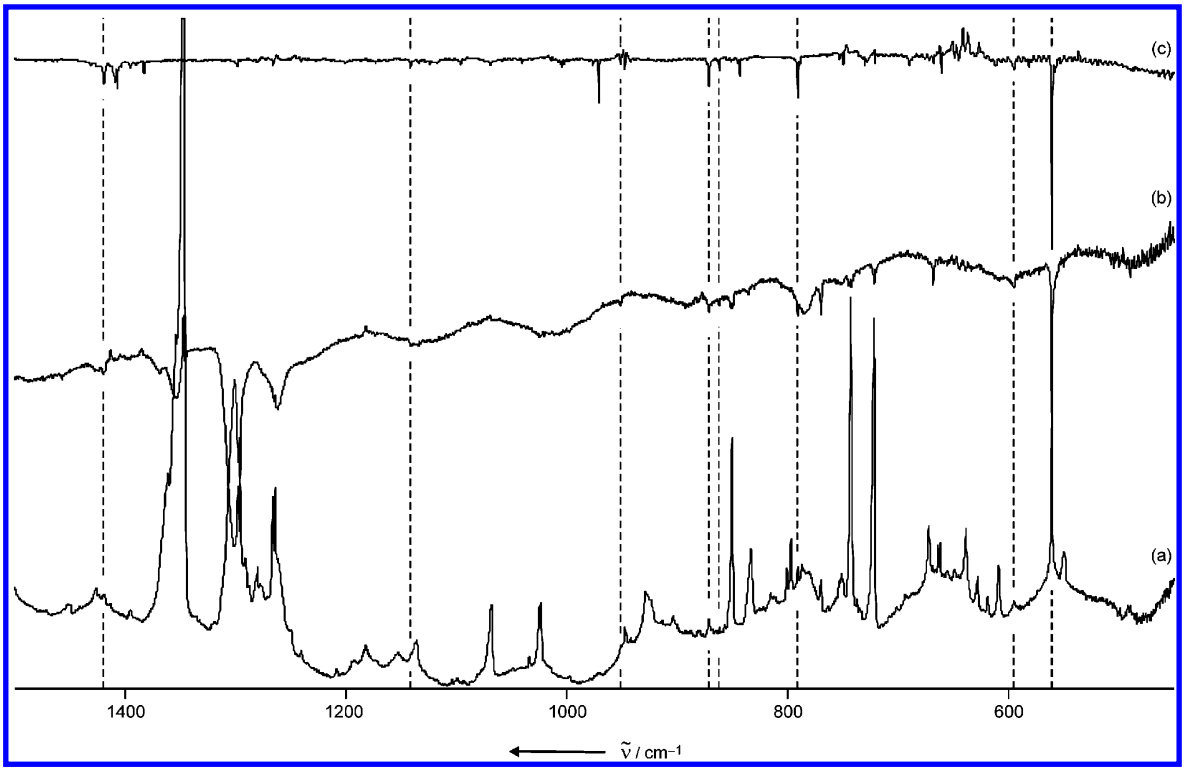

Figure 3. (a) IR spectrum of a matrix containing the FVP products of **21**. (b) Difference spectrum; bands pointing downward decrease in intensity upon irradiation ($\lambda = 254$ nm) of a matrix containing the FVP products of **21**. (c) Difference spectrum; bands pointing downward decrease in intensity upon irradiation of a matrix containing the FVP products of **20**.

Table 1. IR Spectroscopic Data of 3,5-Pyridyne (**3**)

mode	symmetry	$\tilde{\nu}_{exp}$ (cm^{-1})[a]	$I_{exp,rel}$[a]	$\tilde{\nu}_{calcd}$ (cm^{-1})[b]	I_{calcd} (km mol^{-1})[b]
1	*b*1			342.5	0
2	*a*1			354.3	26
3	*a*2			537.2	0
4	*b*2	560.5	100	537.6	130
5	*b*1	595.0	20	580.4	22
6	*b*1	790.5	25	782.6	21
7	*a*1	861.5	5	852.8	5
8	*b*1	871.0	10	864.9	17
9	*a*2			870.2	0
10	*b*2	951.0	5	936.5	8
11	*a*1			1058.3	0
12	*a*1	1141.0	5	1120.1	8
13	*b*2			1180.2	1
14	*b*2			1226.9	1
15	*b*2			1291.9	1
16	*a*1			1373.0	0
17	*b*2	1418.5	10	1417.2	47
18	*a*1	*c*		1684.4	11

[a] Argon, 10 K. [b] BLYP/cc-pVTZ. [c] Not assigned due to the low signal-to-noise ratio in this spectral region.

has been reported upon FVP of other pyridine derivatives in the same temperature range,[29d,e] and the 947.0 cm^{-1} absorption is also observed upon pyrolysis of 2,6-diiodopyridine at 675 °C [Figure 2S; the structurally related (*E*)-**10** has a strong and characteristic absorption at 942.0 cm^{-1} that allows us to distinguish it from the (*Z*)-isomer]. As expected, all signals associated with **3** and **22** are absent from the IR spectra of the pyrolysate of the 2,6-diiodo compound. The species formed photochemically from **3** and **22** is characterized by a very strong absorption at 3320.5 cm^{-1}, and the most reasonable candidates are (*Z*)-**23** or (*Z*)-**24**. The latter compound possesses two intense signals in the ≡C−H stretching region (3393 and 3406 cm^{-1}, unscaled at the BLYP/cc-pVTZ level), whereas only one signal (3394 cm^{-1}) is expected for (*Z*)-1-aza-hex-3-ene-1,5-diyne. On this basis, we tentiatively identify (*Z*)-**23** as the photoproduct of **3**. High-resolution matrix IR data of acyclic C_5H_3N isomers (a prerequisite for more reliable assignments), although very desirable, are not yet available in the literature. Efforts into this direction are currently under way in our laboratory.

Molecular Structure of 3,5-Pyridyne. The structure of **3** has been calculated with several DFT methods, and the distances R_{C3C5} of the radical centers are summarized in Table 2. Analogous to **1**, hybrid functionals predict a bicyclic form, whereas pure GGA (generalized gradient approximation) functionals lead to a monocyclic geometry for **3**.

In a previous study, we investigated the structure of **1** by a series of constraint geometry optimizations with frozen distances R_{C1C3} between the radical centers at the B3LYP and CASSCF levels.[15a] By varying the separation of the dehydrocarbons (step size 1−5 pm), potential energy curves for the cyclization reaction were obtained. Subsequently, high-level single point calculations [MR-CI, CAS-RS2, CAS-RS3, CCSD(T), and BCCD(T), cf., Experimental Section] have been carried out for a large number of structures obtained in this way. It has been demonstrated that the resulting potential energy curves are almost parallel for both sets of geometries, with the (U)B3LYP structures being slightly lower in energy. Following these lines, we investigated the structure of **3** at the above-mentioned levels of theory for (U)B3LYP/cc-pVTZ optimized geometries with frozen distances R_{C3C5}. In all cases, the lowest energy structure is found at $R_{C3C5} = 200 \pm 5$ pm (Figure 4). Thus, C5H by N replacement in **1** reduces the distance of the dehydrocarbons by 5−7 pm (in

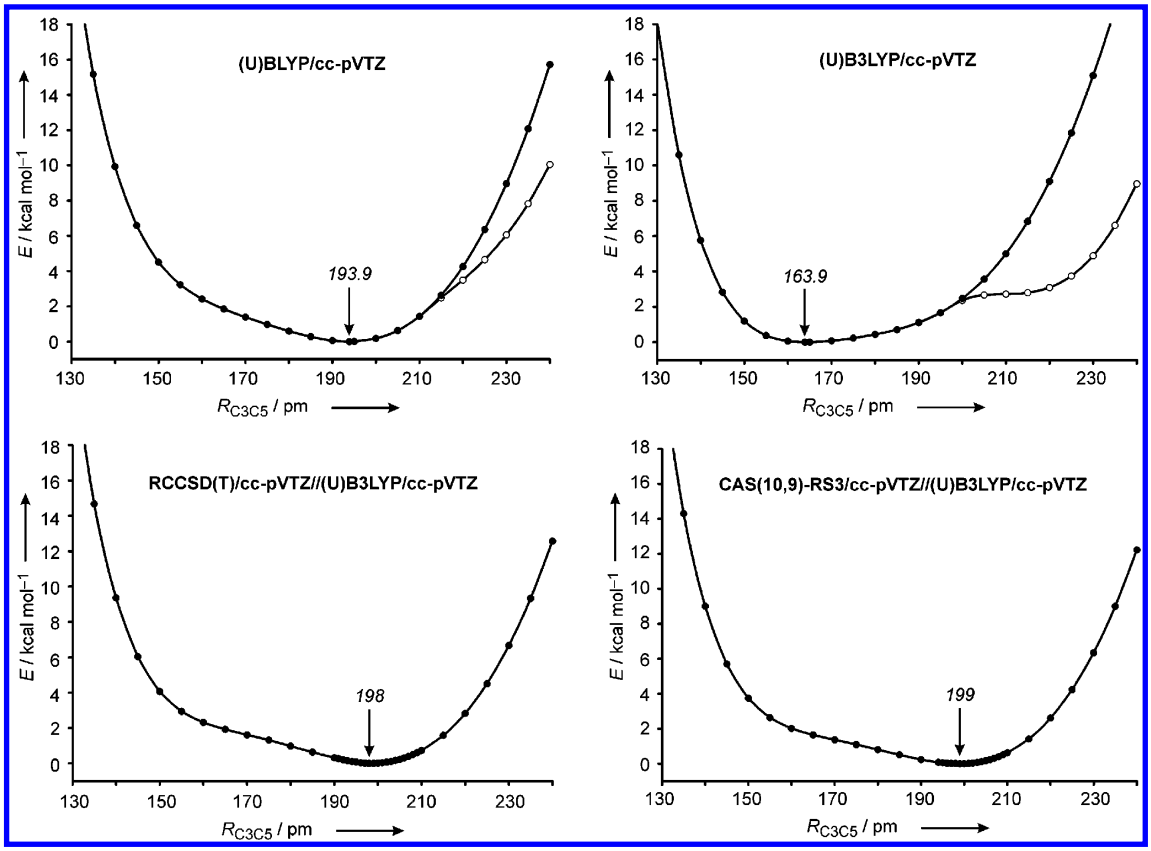

Figure 4. Energy profiles for the cyclization of 3,5-pyridyne (**3**) (energy as a function of the distance of the radical centers) calculated at different levels of theory.

Table 2. Distances *R* of the Radical Centers in *meta*-Benzyne (**1**) and 3,5-Pyridyne (**3**) in pm; Values in Parentheses Give Changes in *R* Due to CH by N Replacement

	1			**3**		
method	cc-pVDZ	cc-pVTZ	cc-pVQZ	cc-pVDZ	cc-pVTZ	cc-pVQZ
B3PW91	157.3	156.2	156.2	159.9 (+2.6)	158.3 (+2.1)	158.3 (+2.1)
B3LYP	161.5	160.3	160.4	166.3 (+4.8)	163.9 (+3.6)	163.9 (+3.5)
BPW91	187.8	184.3	182.2	176.8 (−11.0)	172.7 (−11.6)	172.0 (−10.2)
BLYP	202.1	199.7	199.5	196.2 (−5.9)	193.9 (−5.8)	193.6 (−5.9)
BCCD(T)[a]	211 ± 1	204 ± 1	203 ± 1	202 ± 1 (−9)	198 ± 1 (−6)	197 ± 1 (−6)
RCCSD(T)[a]	211 ± 1	205 ± 1	203 ± 1	203 ± 1 (−8)	198 ± 1 (−7)	198 ± 1 (−5)
CAS-RS3[a]	211 ± 1	205 ± 1	203 ± 1	204 ± 1 (−7)	199 ± 1 (−6)	196 ± 1 (−7)
CAS-CISD+Q[a]	213 ± 1	207 ± 1	206 ± 1	206 ± 1 (−7)	202 ± 1 (−5)	
CAS-CISD[a]	215 ± 1	210 ± 1	209 ± 1	209 ± 1 (−6)	206 ± 1 (−4)	
CAS-RS2[a]	215 ± 1	210 ± 1	209 ± 1	208 ± 1 (−7)	204 ± 1 (−6)	203 ± 1 (−6)

[a] Lowest energy structure calculated for (U)B3LYP/cc-pVTZ optimized geometries with frozen distances *R*. See text for details.

pyridine **31**, the corresponding distance is 2−3 pm smaller than in benzene **18** at all DFT levels considered in this work, cf. Figure 5).[15]

This trend is reproduced correctly at the BLYP level, whereas the geometries fully optimized with the hybrid methods deviate even qualitatively and predict a slightly increased separation and an overall bicyclic structure. Given the flatness of the potential energy surface along the interradical distance coordinate, a detailed examination of this point might seem irrelevant; however, small structural changes have been used to rationalize substituent effects in a series of substituted *meta*-benzynes;[34] therefore, the ability of different methods to account for systematic changes within this class of compounds is of interest.

The measured IR spectrum of **3** is compared to the vibrational spectra calculated with different DFT methods in Figure 6. Good overall agreement between experiment and the theory is found for the BLYP functional, the only exception being mode 17, for which the calculated intensity is higher than the measured one, and mode 18 that could not be detected in the IR spectra as the low signal-to-noise ratio in this spectral region hampers the identification of very weak absorptions. In contrast, the patterns calculated with the other functionals differ considerably from the observed spectrum and hardly allow any correlation with experiment.

All in all, the distance of the radical centers in **3** is around 200 pm and only slightly smaller than in the parent *meta*-benzyne (**1**). The BLYP calculated data are in good agreement, with both the measured IR spectrum and the structure calculated with highly correlated ab initio methods.

(34) (a) Johnson, W. T. G.; Cramer, C. J. *J. Phys. Org. Chem.* **2001**, *14*, 597. (b) Johnson, W. T. G.; Cramer, C. J. *J. Am. Chem. Soc.* **2001**, *123*, 923.

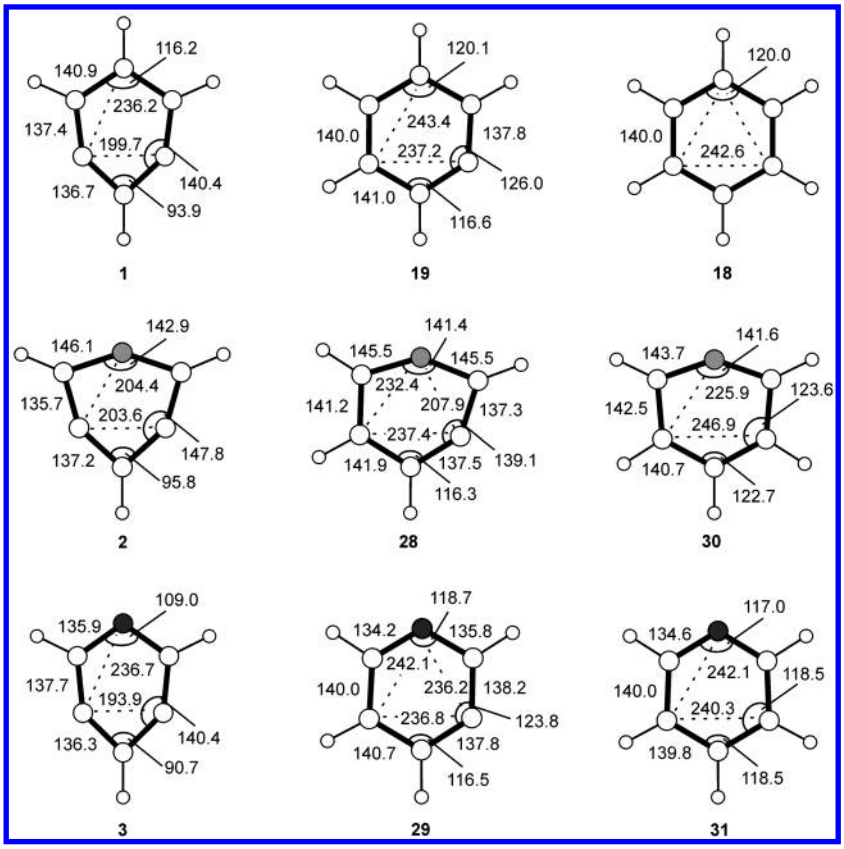

Figure 5. Structures of biradicals **1**−**3** and of the corresponding monoradicals and parent arenes calculated at the BLYP/cc-pVTZ level of theory.

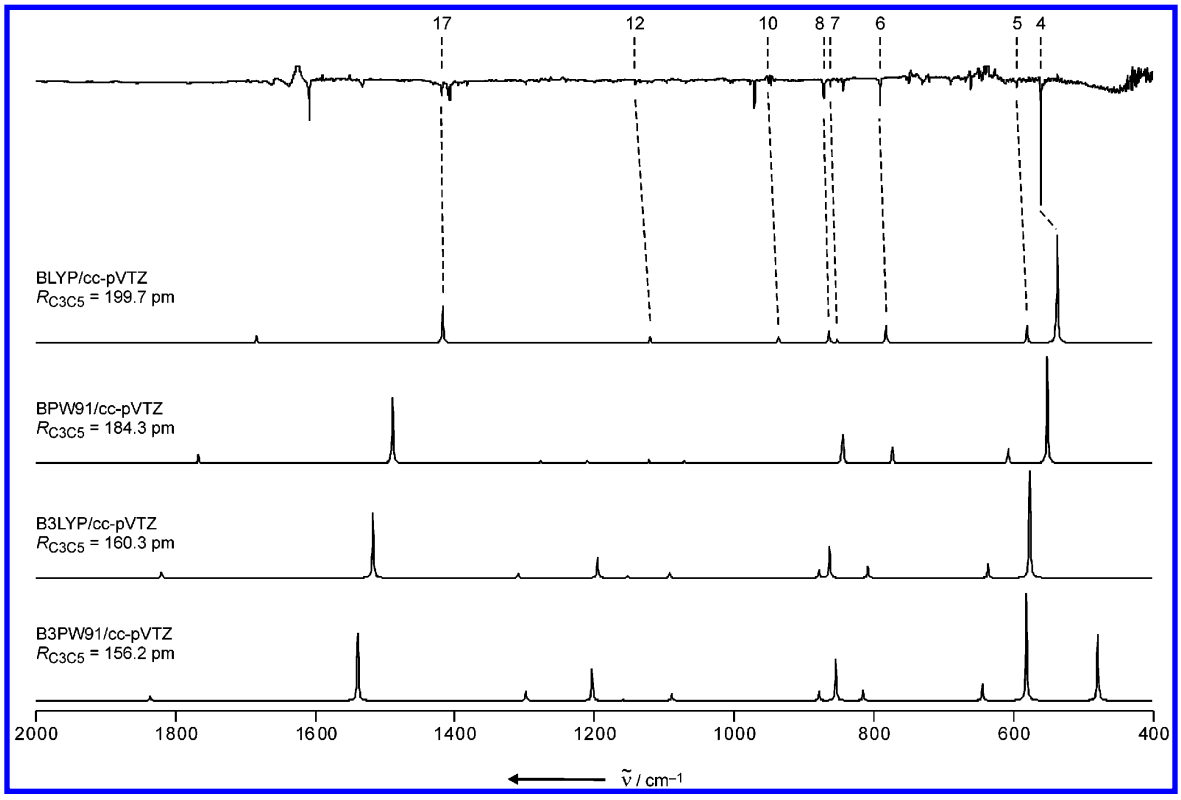

Figure 6. Comparison of the measured IR spectrum of **3** with the vibrational spectra calculated with different DFT methods.

Electronic Structure of 3,5-Pyridyne. To clarify the effect of the nitrogen lone pair on the electronic structure of 3,5-pyridyne, we calculated the energy differences between the lowest energy singlet and triplet states (ΔE_{ST}) of **1** and **3** at high levels of theory (Table 3). For **1**, CASSCF(8,8) predicts a singlet−triplet splitting considerably smaller (13 kcal mol^{-1}) than the experimentally determined value of 21.0 ± 0.3 kcal mol^{-1}.[35] Inclusion of dynamic electron correlation stabilizes the

Table 3. Singlet−Triplet Energy Splittings [$E_0(^3B_2) - E_0(^1A_1)$] in *meta*-Benzyne (**1**) and 3,5-Pyridyne (**3**) in kcal mol^{-1}; Electronic Contributions [$E_e(^3B_2) - E_e(^1A_1)$] Are Given in Parentheses

	1			**3**		
method	cc-pVDZ	cc-pVTZ	cc-pVQZ	cc-pVDZ	cc-pVTZ	cc-pVQZ
B3PW91	15.8 (15.5)	16.6 (16.4)	16.7 (16.5)	11.1 (10.7)	12.1 (11.6)	12.3 (11.8)
B3LYP	14.0 (13.6)	14.8 (14.4)	15.0 (14.6)	9.2 (8.6)	10.2 (9.6)	10.4 (9.8)
BPW91	19.7 (19.2)	20.1 (19.6)	20.2 (19.7)	12.9 (12.2)	13.6 (12.9)	13.7 (13.1)
BLYP	19.5 (19.3)	19.9 (19.7)	19.9 (19.7)	11.5 (11.2)	12.2 (11.9)	12.4 (12.0)
CAS-SCF[a]	11.8 (11.7)	12.9 (12.7)	13.0 (12.8)	9.3 (8.9)	10.3 (9.9)	10.4 (10.0)
CAS-RS2[a]	17.0 (16.9)	19.5 (19.3)	20.2 (20.0)			
CAS-RS3[a]	16.5 (16.3)	19.0 (18.9)	19.7 (19.5)			
CAS-CISD[a]	16.4 (16.2)	18.6 (18.5)	19.1 (18.9)	13.5 (13.1)	15.7 (15.4)	16.2 (15.8)
CAS-CISD+Q[a]	17.3 (17.1)	20.0 (19.8)	20.5 (20.4)	14.4 (14.0)	17.1 (16.7)	17.6 (17.2)
exp[b]			21.0 ± 0.3			NA

[a] (U)BLYP/cc-pVTZ geometries and ZPVE corrections. [b] Ref 35.

singlet relative to the triplet state. Particularly good agreement with experiment is obtained at the MR-CI level (20.5 kcal mol^{-1}), provided that sufficiently large basis sets (cc-pVQZ) are used and higher order correlation effects are accounted for by the Davidson correction scheme. Among the DFT methods, BPW91 and BLYP give energy differences around 20 kcal mol^{-1}, whereas admixture of exact exchange (B3PW91, B3LYP) lowers these values by 4−5 kcal mol^{-1}. For **3**, MR-CI predicts a decrease of the singlet−triplet splitting by 3 kcal mol^{-1} as compared with **1**, in good agreement with previous investigations.[11,12] All DFT methods perfom somewhat worse in this case and underestimate ΔE_{ST} of **3** by 4 (BPW91) to 8 kcal mol^{-1} (B3LYP) as compared to the MR-CI benchmark data.

The effect of heteroatomic substitution on the stability of *meta*-benzynes can be estimated on the basis of BSE, defined according to isodesmic eq 2 (cf. refs 36 and 37). These provide a measure for the stabilization or destabilization involved when the two radical centers interact within the same molecule. A positive value indicates stabilization, and a negative value indicates destabilization with respect to a hypothetical noninteracting biradical model system;[36] it is immediately obvious that the BSE is equivalent to the difference between the first and the second C−H BDE in the corresponding arene. An alternative approach that avoids reference to the monoradical is given by eq 3, defining what we would like to call the stabilization energy (SE).

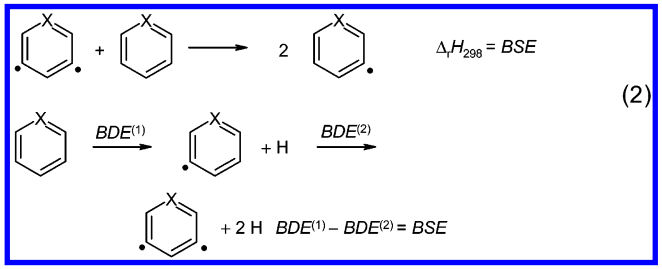

(2)

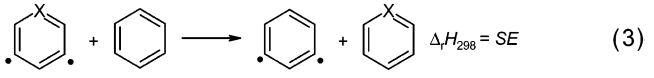

(3)

The (U)BLYP/cc-pVTZ calculated BSEs and SEs of *meta*-benzyne (**1**), 3,5-borabenzyne (**2**), and 3,5-pyridyne (**3**) are listed in Table 4. The BSE of **1** amounts to 16.6 kcal mol^{-1} and

Table 4. Different Measures (Enthalpies at 298 K in kcal mol^{-1}) for the Influence of Heteroatomic Substitution on the Stability of **1**

system	BDE$^{(1)a}$	BDE$^{(2)a}$	BSE[a]	SE[b]
X = B	97.7	71.3	26.4	28.3
X = CH	107.0	90.4	16.6	0.0
X = N	106.3	94.1	12.3	−3.0

[a] Cf. eq 2. [b] According to eq 3.

underlines the significant coupling of the formally unpaired electrons. According to both schemes described above, **3** is approximately 3−4 kcal mol^{-1} less stable than *meta*-benzyne. In contrast, **2** benefits from a significant stabilization (SE = 28 kcal mol^{-1}), and the structure of this molecule is indicative of strong two electron, three center interaction with very similar C−C and C−B distances (Figure 5), coming close to the D_{3h} structure of **4** (R_{C1C3} = 200.3 pm).

Whereas the considerable stabilization of **2** may be expressed by the term in-plane aromaticity, the overall effect of the nitrogen lone pair on the coupling of the formally unpaired electrons in **3**, as measured by the distance of the radical centers, the stability, and the singlet−triplet splitting, is rather small. Analogous to tridehydrobenzene (**17**),[28] **3** is best described as a *meta*-benzyne moiety interacting only weakly with a nitrogen atom on the opposite side of the ring. This view is further supported by comparison of the frontier molecular orbitals of **1**−**3**, shown in Figure 7.

The highest occupied (HOMO) and lowest unoccupied molecular orbitals (LUMO) of **1** and **3** are almost indistinguishable in the region of the dehydrocarbons, and the occupation numbers of the corresponding MCSCF natural orbitals (NOON) are very similar (note that the distance of the radical centers in **3** is slightly smaller than in **1**, leading to larger NOON of the HOMO and lower NOON of the LUMO of **3**). The lone pair, on the other hand, is largely localized on the nitrogen atom. In contrast, the frontier molecular orbitals of **2** are those of a σ-allylic system with significantly increased NOON of the bonding three center HOMO.

We also investigated the magnetic properties of **1**−**3** and of the corresponding parent arenes at the BLYP/cc-pVTZ level. Nucleus-independent chemical shifts (NICS)[38] were calculated to access the diamagnetic/paramagnetic effects of the ring currents associated with aromaticity/antiaromaticity.[38,39] Abso-

(35) Wenthold, P. G.; Squires, R. R.; Lineberger, W. C. *J. Am. Chem. Soc.* **1998**, *120*, 5279.

(36) (a) Wierschke, S. G.; Nash, J. J.; Squires, R. R. *J. Am. Chem. Soc.* **1993**, *115*, 11958. See also (b) Cramer, C. J.; Nash, J. J.; Squires, R. R. *Chem. Phys. Lett.* **1997**, *277*, 311.

(37) Lindh, R.; Bernhardsson, A.; Schütz, M. *J. Phys. Chem. A* **1999**, *103*, 9913.

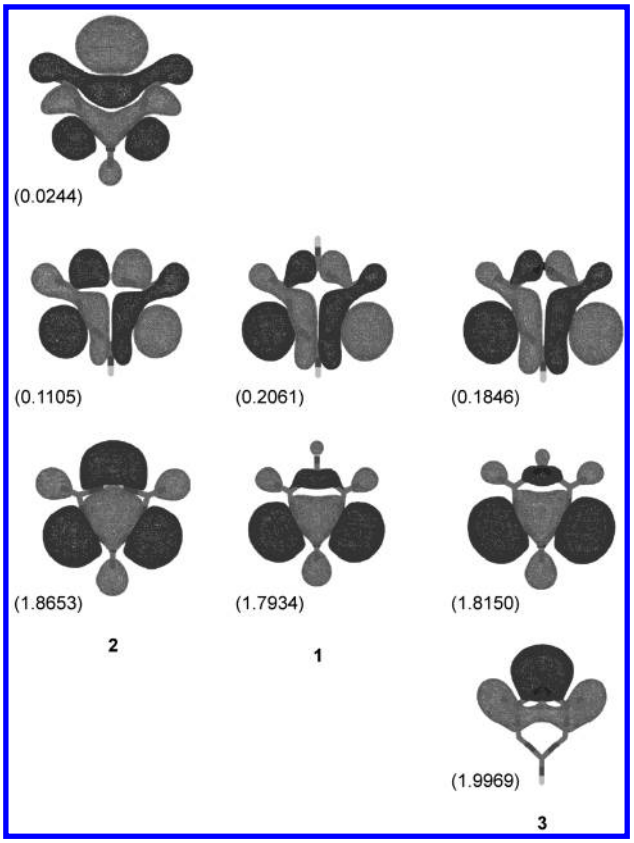

Figure 7. Frontier molecular orbitals of biradicals **1**−**3** (CASSCF canonical orbitals) and occupation numbers of the corresponding natural orbitals.

Table 5. NICS of **1**−**3** and of the Parent Hydrocarbons Calculated at the BLYP/cc-pVTZ Level of Theory at the (3,+1) Ring Critical Point [NICS(0)] and 100 [NICS(1)] or 200 pm [NICS(2)] above the Molecular Plane

molecule	NICS(0)	NICS(1)	NICS(2)
meta-benzyne (**1**)	−11.8	−11.1	−4.8
benzene (**18**)	−7.8	−9.9	−5.0
3,5-borabenzyne (**2**)	−33.4	−17.3	−6.3
borabenzene (**30**)	−12.2	−9.6	−4.1
3,5-pyridyne (**3**)	−5.2	−9.6	−4.4
pyridine (**31**)	−6.6	−9.8	−4.9

lute chemical shifts within the plane of cyclic molecules are a measure of the extent of cyclic electron delocalization only when the radii of the systems are sufficiently large, so that local shielding effects are negligible.[38a,c] It has, therefore, been recommended to calculate NICS(1) values 100 pm above the ring plane, where local contributions to the total chemical shift are considerably weaker than ring current effects.[38a,c] The computed NICS(0), NICS(1), and NICS(2) values of **1**−**3** are compared to those of the parent systems in Table 5.

NICS(0) refers to the (3,+1) ring critical point[40] (instead of the ring center usually chosen), i.e., the point of lowest electron density within the molecular plane. Following the recommendations mentioned above, we concentrate on NICS(1) here. Almost identical values between −9.6 and −9.9 are calculated for benzene (**18**), borabenzene (**30**), and pyridine (**31**). Removing two hydrogens from **18** leads to slightly more negative NICS for *meta*-benzyne (as well as for the *ortho*- and *para*-isomers), as discussed in detail previously.[41] Chemical shifts for **3** are almost identical to that of pyridine, indicating the absence of any paramagnetic ring currents that may be associated with antiaromaticity. On the other hand, a large negative NICS for **2** is calculated, justifying the notion of in-plane aromaticity in this case.

Rearrangements of 3,5-Pyridyne. Rearrangements on the C_6H_4 potential energy surface have been investigated in several studies employing the B3LYP functional.[4b,18,21] To compare the chemistry of benzynes and pyridynes at consistent levels of theory, we reinvestigated the most important intramolecular reactions of **1** using the BCCD(T)/cc-pVTZ//(U)BLYP/cc-pVTZ and CCSD(T)/cc-pVTZ//(U)BLYP/cc-pVTZ methods. A potential energy diagram for the rearrangements considered in this work is shown in Figure 8.

The *meta*- to *para*-benzyne interconversion proceeds by a nonplanar transition state structure TS_{1-11} and requires an activation energy of approximately 60 kcal mol^{-1} (Figure 3S), which is similar to the degenerate [1,2]H shift in the phenyl radical.[42] A related hydrogen shift mechanism leading to *ortho*-benzyne (**32**) is characterized by an even higher barrier[43] (Figure 4S), but a second transition state with a bicyclic C_s structure could be located that is less stable than *meta*-benzyne by 58 kcal mol^{-1} and leads to fulvenediyl **33** (Figure 5S). This, in turn, rearranges with a very small barrier to **32**.[44] In accordance with our previous discussion on the basis of B3LYP calculations and experimental observations,[18] all of these reactions are unlikely to occur under FVP conditions, however, because a lower energy transition state TS_{1-Z10} was identified that leads to (*Z*)-hex-3-ene-1,5-diyne **10**. This pathway is also favored entropically ($T\Delta S_{298}^{\#}$ at 298 K is 2.62 kcal mol^{-1} for the **1** → (*Z*)-**10** ring-opening, but only 0.44 kcal mol^{-1} for the hydrogen shift **1** → **11** at the (U)BLYP/cc-pVTZ level), and should, therefore, prevail in high-temperature processes. Details of this unusual rearrangement are given in Figure 9, which shows several structures along the intrinsic reaction coordinate (IRC).[45] The potential energy surface in the region of transition state TS_{1-Z10} is extremely flat, and the imaginary frequency (148*i* cm^{-1}) is small. In the early stage of this process, the ring opens and the acetylenic moiety forms, whereas the hydrogen migration takes place mainly after passage through the transition state. In agreement with prior calculations,[18] no vinylidene exists as a stationary point.

Several other mechanisms for the reaction **1** → (*Z*)-**10** can be envisaged but are less likely due to the high energy of the

(38) (a) Schleyer, P. v. R.; Manoharan, M.; Wang, Z.-X.; Kiran, B.; Jiao, H.; Puchta, R.; Hommes, N. J. R. van E. *Org. Lett.* **2001**, *3*, 2465. (b) Schleyer, P. v. R.; Jiao, H.; Hommes, N. J. R. van E.; Malkin, V. G.; Malkina, O. L. *J. Am. Chem. Soc.* **1997**, *119*, 12669. (c) Schleyer, P. v. R.; Maerker, C.; Dransfeld, A.; Jiao, H.; Hommes, N. J. R. van E. *J. Am. Chem. Soc.* **1996**, *118*, 6317.
(39) For general reviews on aromaticity criteria, see, for example (a) Special Issue on Aromaticity. Schleyer, P. v. R., Ed. *Chem. Rev.* **2001**, *101*, 1115. (b) Minkin, V. I.; Glukhovtsev, M. N.; Simkin, B. Y. *Aromaticity and Antiaromaticity*; Wiley: New York, 1994.
(40) (a) Popelier, P. *Atoms in Molecules*; Prentice Hall: Harlow, 2000. (b) Bader, R. W. F. *Chem. Rev.* **1991**, *91*, 893. (c) Bader, R. W. F. *Atoms in Molecules: A Quantum Theory*; Clarendon Press: Oxford, 1990.
(41) De Proft, F.; Schleyer, P. v. R.; Lenthe, J. H. van; Stahl, F.; Geerlings, P. *Chem. Eur. J.* **2002**, *8*, 3402.
(42) Brooks, M. A.; Scott, L. T. *J. Am. Chem. Soc.* **1999**, *121*, 5444.
(43) In ref 4b, it has been reported that this transition state leads to a high-energy intermediate [at B3LYP/6-31G(d,p)]. Our IRC calculations reveal, however, that TS_{1-32} leads directly to *ortho*-benzyne at the (U)BLYP/cc-pVTZ level (cf., Figure 4S) without passage through an additional intermediate.
(44) There is no experimental evidence for *meta*- to *ortho*-benzyne conversion under FVP conditions. Recently, M. Jones et al. reported the rearrangement of a substituted *ortho*-benzyne to the *meta*-isomer by migration of a phenyl group. Blake, M. E.; Bartlett, K. L.; Jones, M., Jr. *J. Am. Chem. Soc.* **2003**, *125*, 6485.
(45) (a) Gonzalez, C.; Schlegel, H. B. *J. Phys. Chem.* **1990**, *94*, 5523. (b) Gonzalez, C.; Schlegel, H. B. *J. Chem. Phys.* **1989**, *90*, 2154.

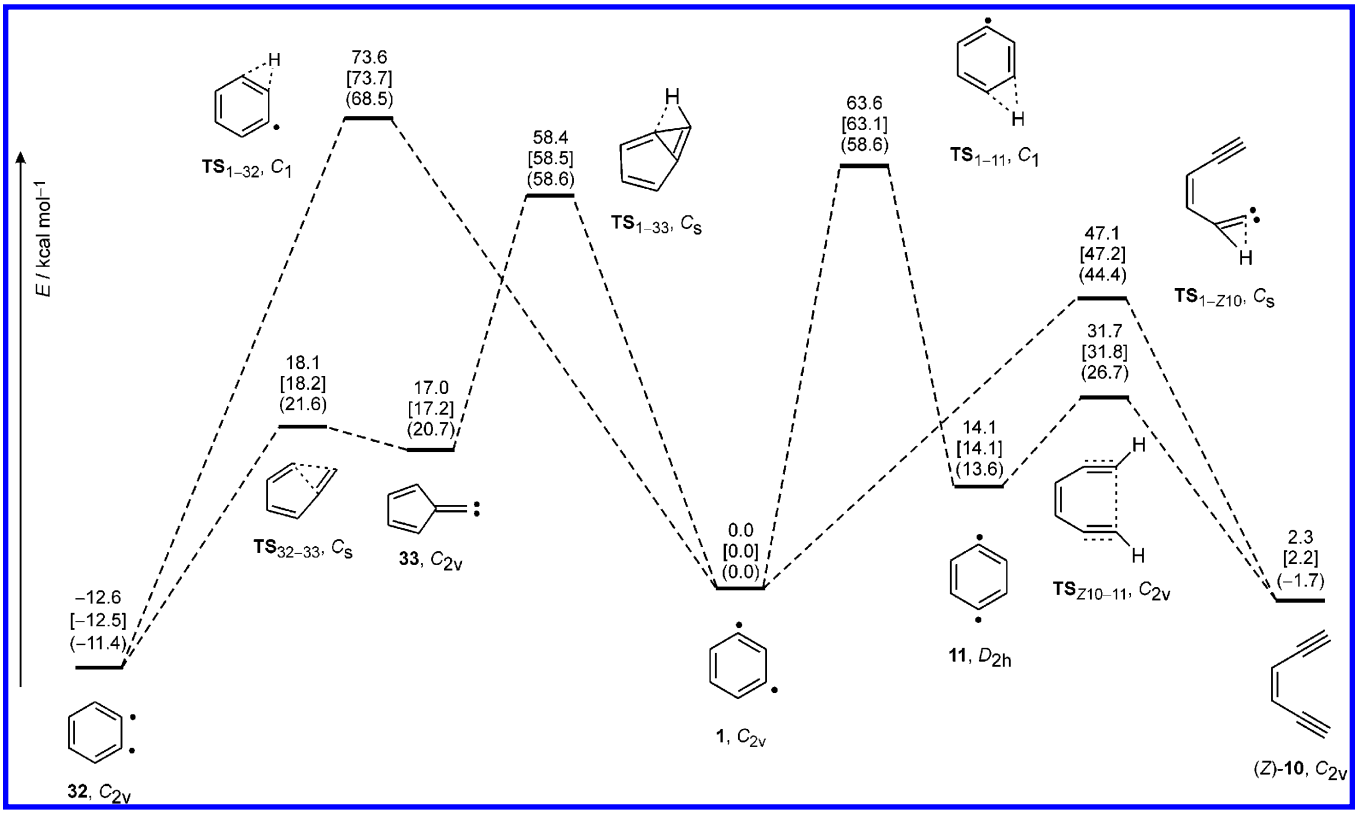

Figure 8. Potential energy diagram for rearrangements of *meta*-benzyne calculated at the BCCD(T)/cc-pVTZ//(U)BLYP/cc-pVTZ [CCSD(T)/cc-pVTZ//(U)BLYP/cc-pVTZ] ((U)BLYP/cc-pVTZ) level of theory. All values include ZPVE corrections ((U)BLYP/cc-pVTZ).

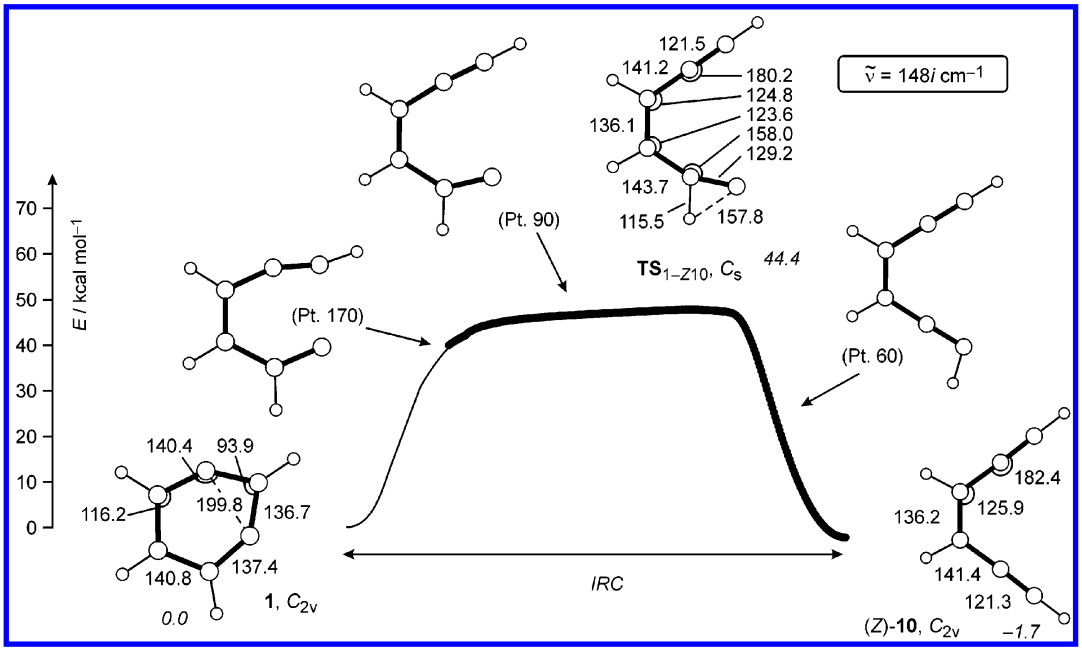

Figure 9. Structures along the IRC for the ring-opening of *meta*-benzyne (BLYP/cc-pVTZ). Energies (E_0) relative to **1** are given in italics.

intermediates involved. The direct formation of fulvene-1,4-diyls **35** from **1** has been shown to require large activation energies and is not considered any further here (Scheme 3).[18] Given the recent interest in these five-membered biradicals,[46] however, it should be mentioned that the (*E*)-isomer does not correspond to a stationary point on the UBLYP/cc-pVTZ potential energy surface and is only found as an intermediate when small basis sets are employed.[46] Formation of the isomeric fulvene-1,3-diyls (*Z*)-**34** and (*E*)-**34** has not yet been discussed in the literature. As these species are already 5−6 kcal mol^{-1} higher in energy than TS_{1-Z10} (Table 6), they can be excluded as intermediates in the FVP process.

Another group of rearrangements is initiated by breaking the C4−C5 bond of *meta*-benzyne (instead of the C1−C2 bond, leading to TS_{1-Z10}). These mechanisms all involve high-energy

(46) (a) Prall, M.; Wittkopp, A.; Schreiner, P. R. *J. Phys. Chem. A* **2001**, *105*, 9265. (b) Alabugin, I. V.; Manoharan, M. *J. Am. Chem. Soc.* **2003**, *125*, 4495.

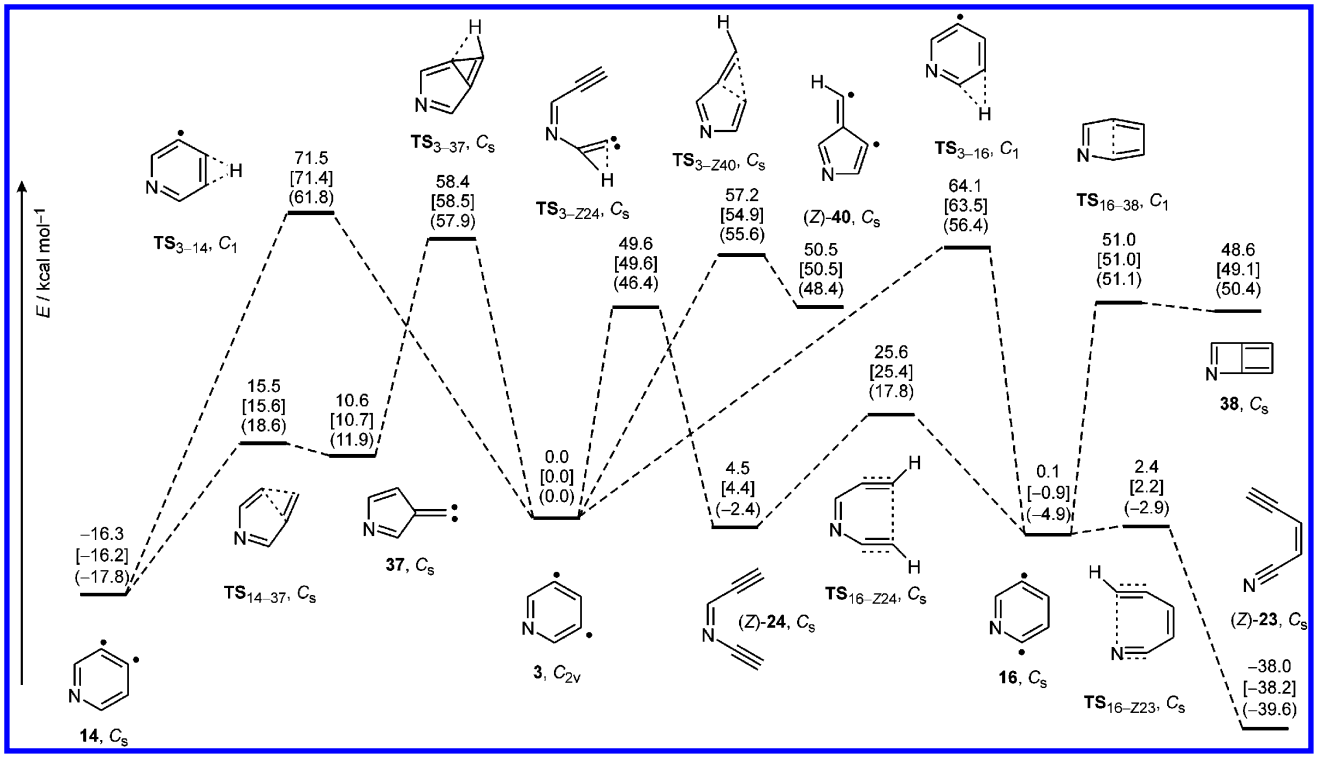

Figure 10. Potential energy diagram for rearrangements of 3,5-pyridyne calculated at the BCCD(T)/cc-pVTZ//(U)BLYP/cc-pVTZ [CCSD(T)/cc-pVTZ//(U)BLYP/cc-pVTZ] ((U)BLYP/cc-pVTZ) level of theory. All values include ZPVE corrections ((U)BLYP/cc-pVTZ).

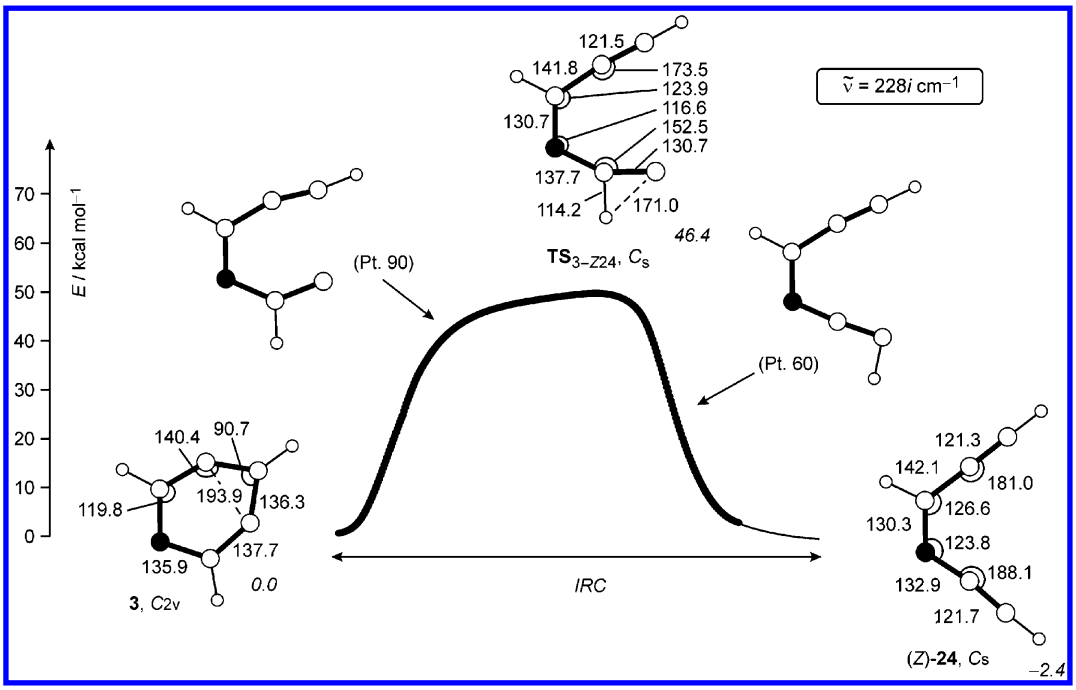

Figure 11. Structures along the IRC for the ring-opening of 3,5-pyridyne (BLYP/cc-pVTZ). Energies (E_0) relative to **3** are given in italics.

structures (e.g., carbene **36**, first suggested by Chen in 1996,[7b] is 70−80 kcal mol^{-1} less stable than **1**, Scheme 4) and, therefore, will not be discussed in detail here. An important point, however, relates to the experimentally observed formation of the (*E*)-enediyne. One might argue that the formation of this species at comparatively low temperatures (550−600 °C) is indicative of an additional intermediate that, like **36**, could lead to (*Z*)-**10** and (*E*)-**10** independently. To clarify this point, we would like to stress that cis−trans isomerization of pure (*Z*)-**10** takes place already at temperatures around 500 °C under the conditions employed in our experiments.[32c] Thus, (*Z*)-**10** is most likely the primary product, formed directly from **1**, and subsequently equilibrates with the (*E*)-isomer.

A potential energy diagram for rearrangements of 3,5-pyridyne (**3**) is given in Figure 10. The barriers for the hydrogen migration mechanisms leading to **14** or **16** are similar to their all-carbon analogues (Figures 6S and 7S). In line with our earlier studies on *meta*-benzyne,[18] there are no indications for the formation of the more stable *ortho*-isomer under FVP conditions (Table 7). The ring-opening, hydrogen shift mechanism leading

Scheme 3

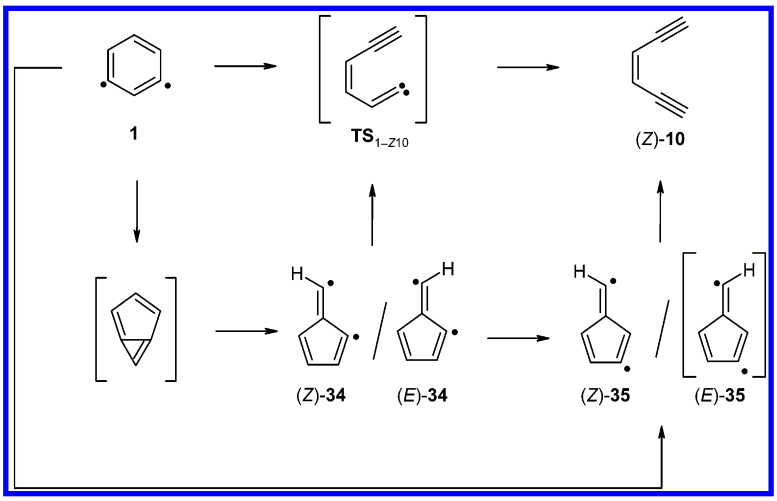

Table 6. Energies of Various Minima and Transition States on the C_6H_4 Potential Energy Surface in kcal mol^{-1} Relative to *meta*-Benzyne; T_1 Diagnostics (CCSD), $\langle S^2 \rangle$ Expectation Values (UBLYP), and Zero-Point Vibrational Energies (UBLYP) Are Given for Comparison

structure	state	$E_{(U)BLYP}$	ZPVE	$\langle S^2 \rangle$	$E_{CCSD(T)}$[a]	T_1[a]	$E_{BCCD(T)}$[a]	E_{MRCI}[a]
1[b]	$^1A_1$	0.0	44.85	0.000	0.0	0.015	0.0	0.0
(*Z*)-**10**	$^1A_1$	0.3	42.79	0.000	4.3	0.013	4.3	
(*E*)-**10**	^1A_g	−0.3	42.67	0.000	3.9	0.013	3.9	
11	^1A_g	13.9	44.52	0.768	14.5	0.019	14.5	15.1
32	$^1A_1$	−12.3	45.74	0.000	−13.4	0.013	−13.5	−14.0
33	$^1A_1$	21.5	44.10	0.000	17.9	0.016	17.7	18.4
(*Z*)-**34**	$^1A'$	55.8	43.18	0.954	53.9	0.043	56.1	54.2
(*E*)-**34**	$^1A'$	56.3	43.03	0.982	49.4	0.070	57.5	55.5
(*Z*)-**35**	$^1A'$	52.3	42.47	0.807	25.9	0.107	51.3	51.2
36	^1A	69.1	40.20	0.636	81.5	0.020	81.4	
41	^1A_g	48.1	43.82	0.000	46.9	0.013	46.8	
TS_{1-Z10}	$^1A'$	48.6	40.66	0.000	51.4	0.014	51.3	
TS_{1-11}	^1A	62.4	41.03	0.000	66.9	0.036	67.5	
TS_{1-32}	^1A	71.7	41.73	0.000	76.8	0.027	76.7	
TS_{1-33}	$^1A'$	61.7	41.72	0.000	61.6	0.016	61.5	
TS_{Z10-11}	$^1A_1$	29.0	42.56	0.000	34.1	0.017	34.0	
TS_{11-41}	^1A	51.9	43.21	0.000	52.1	0.016	52.0	
TS_{32-33}	$^1A'$	22.7	43.73	0.000	19.4	0.013	19.2	

[a] UBLYP/cc-pVTZ optimized geometries. [b] Absolute energies for this row: $E_{(U)BLYP} = -230.885963$; $E_{CCSD(T)} = -230.456091$; $E_{BCCD(T)} = -230.455781$; and $E_{MRCI} = -230.409049$.

Scheme 4

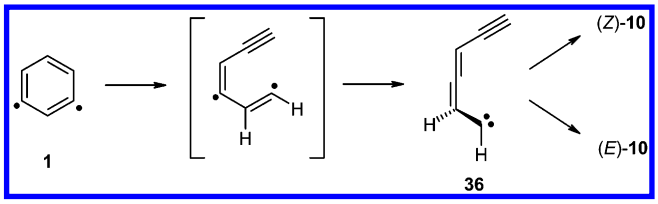

to (*Z*)-**24** requires an activation energy of approximately 50 kcal mol^{-1}, so that the kinetic stability of **3** is even slightly higher than that of **1**. This lowest energy decomposition pathway proceeds similar to the **1** → (*Z*)-**10** rearrangement in a single step without involvement of a vinylidene intermediate (Figure 11).

One can imagine several pathways for the formation of **26** + HCN from **3** or (*Z*)-**24**. Noteworthy, these compounds are not observed in detectable amounts upon FVP of 2,6-diiodopyridine (Figure 2S), which gives (*E*)-**23** (the thermodynamic sink) as the main product (vide supra). Therefore, it seems unlikely that hydrogen cyanide and butadiyne are formed through decomposition of **23**, as proposed in an early investigation.[29d]

Scheme 5

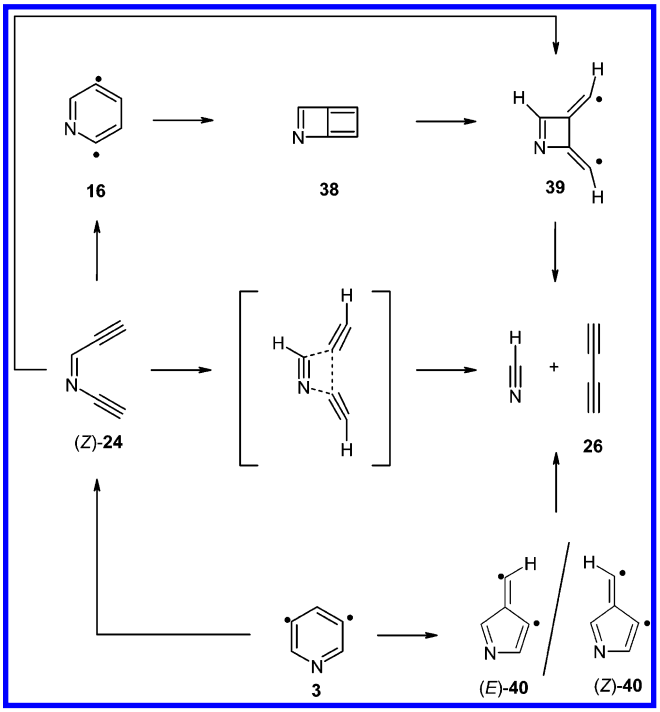

Some plausible mechanisms for the net reaction **3** → **26** + HCN are given in Scheme 5.

Formation of azabutalene (**38**) from **16** requires an activation energy of 52−56 kcal mol^{-1}, considerably more than the 36−39 kcal mol^{-1} barrier for the formation of butalene (**41**) from **11** (Tables 6 and 7).[16b] In addition, the cyclization of **16** is an unlikely event, because the pyridyne easily undergoes a retro-Bergman cyclization to (*Z*)-**23** with a very small and at high temperatures probably vanishing barrier.[8,12] Thus, **16** qualifies as a precursor for **23** but not for the fragmentation products HCN and butadiyne. Biradical **39** is a high-energy species (67 kcal mol^{-1} less stable than **3** at the UBLYP level) and can be excluded as an intermediate in HCN extrusion. On the basis of similar arguments, the involvement of aza-fulvenediyls **40** in the decomposition process of **3** is unlikely, because the former are already comparable in energy to TS_{3-Z24} (Table 7), and the barrier for the **3** → (*Z*)-**40** rearrangement is at least 5 kcal mol^{-1} higher than for the **3** → (*Z*)-**24** ring-opening. However, all

Table 7. Energies of Various Minima and Transition States on the C_5H_3N Potential Energy Surface in kcal mol^{-1} Relative to 3,5-Pyridyne; T_1 Diagnostics (CCSD), $\langle S^2 \rangle$ Expectation Values (UBLYP), and Zero-Point Vibrational Energies (UBLYP) Are Given for Comparison

structure	state	$E_{(U)BLYP}$	ZPVE	$\langle S^2 \rangle$	$E_{CCSD(T)}$[a]	T_1[a]	$E_{BCCD(T)}$[a]	E_{MRCI}[a]
3[b]	$^1A_1$	0.0	37.66	0.000	0.0	0.014	0.0	0.0
12	$^1A_1$	0.8	38.35	0.000	6.6	0.026	6.5	5.1
13	$^1A'$	−12.9	37.94	0.000	−11.1	0.030	−10.5	−11.4
14	$^1A'$	−18.7	38.53	0.000	−17.1	0.017	−17.1	−17.6
15	$^1A'$	−12.9	38.47	0.000	−11.4	0.023	−11.3	−11.7
16	$^1A'$	−4.9	37.71	0.000	−0.9	0.038	0.1	−0.3
(*Z*)-**23**	$^1A'$	−38.5	36.59	0.000	−37.1	0.014	−37.0	
(*E*)-**23**	$^1A'$	−39.2	36.44	0.000	−37.5	0.014	−37.3	
(*Z*)-**24**	$^1A'$	−0.2	35.45	0.000	6.6	0.015	6.7	
(*E*)-**24**	$^1A'$	−0.3	35.18	0.000	7.0	0.015	7.1	
(*Z*)-**25**	$^1A'$	−16.5	36.24	0.000	−15.2	0.015	−15.1	
(*E*)-**25**	$^1A'$	−16.9	36.07	0.000	−15.2	0.015	−15.1	
26/HCN	$^1\Sigma_g^+/^1\Sigma^+$	−1.8	32.55	0.000	4.1	0.014/0.014	4.3	
27/C_2H_2	$^1\Sigma^+/^1\Sigma_g^+$	1.5	32.72	0.000	7.1	0.015/0.013	7.4	
37	$^1A'$	12.4	37.16	0.000	11.2	0.021	11.1	11.7
38	$^1A'$	51.8	36.29	0.000	50.5	0.017	50.0	
(*Z*)-**40**	$^1A'$	49.1	36.20	1.001	52.0	0.026	52.0	49.7
(*E*)-**40**	$^1A'$	49.9	36.11	1.007	53.3	0.030	53.1	51.0
TS_{3-14}	^1A	66.3	33.13	0.007	75.9	0.038	76.0	
TS_{3-16}	^1A	61.0	33.08	0.000	68.1	0.033	68.6	
TS_{3-37}	$^1A'$	61.2	34.40	0.000	61.7	0.015	61.6	
TS_{3-Z24}	$^1A'$	50.3	33.68	0.000	53.6	0.017	53.6	
TS_{3-Z40}	$^1A'$	58.0	35.27	0.474	57.3	0.053	59.6	59.3
TS_{14-37}	$^1A'$	19.8	36.41	0.000	16.8	0.014	16.7	
TS_{16-Z23}	$^1A'$	−1.9	36.67	0.000	3.2	0.025	3.3	
TS_{16-Z24}	$^1A'$	19.9	35.55	0.000	27.5	0.023	27.7	
TS_{16-38}	^1A	53.0	35.77	0.000	52.9	0.015	52.9	

[a] UBLYP/cc-pVTZ optimized geometries. [b] Absolute energies for this row: $E_{(U)BLYP} = -246.932953$; $E_{CCSD(T)} = -246.477854$; $E_{BCCD(T)} = -246.477537$; and $E_{MRCI} = -246.429420$.

attempts to find a feasible route for HCN elimination from **3** or **24** failed so far, and only high-energy structures (more than 60 kcal mol^{-1} above 3,5-pyridyne) could be located for the reverse reaction of HCN with **26**. Therefore, additional experimental (e.g., isotopic labeling) and systematic computational efforts will be necessary, to clarify the mechanism of HCN formation during the FVP experiments described in this work.

Conclusions

3,5-Pyridyne, the second least stable among the six pyridynes, has been generated by FVP of 3,5-diiodopyridine and 3,5-dinitropyridine. The IR spectrum of **3** is well-reproduced at the BLYP level, which predicts a monocyclic structure with a distance between the radical centers close to 200 pm, in good agreement with high-level ab initio calculations. The nitrogen atom in **3** causes only a small perturbation on the electronic structure of *meta*-benzyne that destabilizes the singlet ground state of **3** by 3−4 kcal mol^{-1}. From the calculated magnetic properties and from inspection of molecular orbitals, it can be inferred that a four electron, three center interaction is insignificant within this molecule and that 3,5-pyridyne is best described in terms of a separated *meta*-benzyne moiety and a nitrogen lone pair on the opposite side of the ring. In contrast, a strongly stabilizing two electron, three center interaction is observed for the in-plane aromatic 3,5-borabenzyne.

The title pyridyne is photolabile under matrix isolation conditions and rapidly rearranges upon 254 nm irradiation, presumably to (*Z*)-1-aza-hex-3-ene-1,5-diyne. Among the byproducts of the FVP experiments (*E*)-**23** as well as HCN and butadiyne are the most prominent contaminants. Analogous to the parent *meta*-benzyne, the lowest energy decomposition pathway of **3** is a ring-opening reaction, accompanied by hydrogen migration, leading to (*Z*)-3-aza-hex-3-ene-1,5-diyne. (*E*)-**23** is most likely formed via an aza-Bergman rearrangement of (*Z*)-**24**, followed by cis−trans isomerization of (*Z*)-**23**. Although some mechanisms for HCN extrusion from **3** or (*Z*)-**24** have been considered, a plausible route for this fragmentation has not been identified yet and a more detailed investigation of this point will be the subject of a forthcoming study.

Experimental Section

General. THF was distilled from benzophenone/Na prior to use. Column chromatography was carried out on ICN silica 32−63 (60 Å). NMR spectra were recorded on a Bruker DPX 200; chemical shifts are given relative to TMS: d = doublet, t = triplet, m = multiplet. Mass spectra were measured on Varian MAT CH 5, and IR spectra (KBr) were measured on a Perkin-Elmer 841 IR spectrometer. 2,6-Diiodopyridine was prepared from the corresponding dibromo compound as described previously[47] and purified by 2-fold sublimation.

3,5-Diiodopyridine (20).[48] A solution of *t*-BuLi in hexane (11.8 mL, 1.6 N, 20.0 mmol) was added with stirring to a solution of 3,5-dibromopyridine (1.2 g, 5.0 mmol) in THF (30 mL) at −80 °C in a dry argon athmosphere. After 1 h, iodine (5.1 g, 20.0 mmol) in THF (20 mL) was added. After an additional hour of stirring, the resulting mixture was allowed to warm to room temperature. The solution was poured into 5% $Na_2S_2O_3$ (150 mL) and extracted twice with TBME (200 mL). The combined organic layers were washed with brine and dried ($MgSO_4$). After removal of the solvent, the product crystallized in yellowish needles (1.8 g). The crude product was purified chromatographically (silica gel; CH_2Cl_2/pentane 50:50) to furnish 1.2 g (3.6 mmol, 83.5%) of white needles; mp 170 °C. IR (cm^{-1}, Ar, 10 K): 1533, 1409, 1298, 1096, 1004, 871, 730, 627. ^{1}H NMR (200 MHz, DMSO-d_6): δ_H 8.77 (d, 2H), 8.59 (t, 1H). ^{13}C NMR (100 MHz, DMSO-d_6): δ_C 153.97, 151.18, 95.64. MS (EI, 70 eV) (*m*/*z*, %): 331 (100) [M$^+$], 204 (44), 177 (18), 165 (4), 127 (14), 77 (39), 50 (80).

(47) (a) Newkome, G. R.; Moorfield, C. N.; Sabbaghian, B. *J. Org. Chem.* **1986**, *51*, 953. (b) Newkome, G. R.; Roper, J. M. *J. Organomet. Chem.* **1980**, *186*, 147.
(48) Yamamoto, Y.; Yanagi, A. *Chem. Pharm. Bull.* **1982**, *30*, 1731.

3,5-Dinitropyridine (21).[49] To a stirred solution of 2-chloro-3,5-dinitropyridine (2.0 g, 10.0 mmol) in CH_2Cl_2 (30 mL), hydrazinehydrate (10 mL, 20.0 mmol) was added at 0 °C. After the solution was stirred for 18 h at room temperature, the precipitate was filtered off and washed with CH_2Cl_2 and water. The brownish substance (1.6 g) was heated in aqueous $AgNO_3$ for 3 h. After it was cooled to room temperature, the solution was poured into TBME (250 mL). The organic layer was washed twice with 200 mL of water, twice with 200 mL of aqueous ammonia (25%), and finally with brine and dried ($MgSO_4$). After the solvent was removed, the product crystallized in yellowish needles (1.2 g), which were further purified chromatographically (silica gel; CH_2Cl_2/pentane 50:50) to furnish 900 mg (5.4 mmol, 54.5%) of **21**; mp 106 °C. IR (cm^{-1}, KBr): 3090, 1603, 1589, 1520, 1453, 1339, 1292, 1022, 832, 722. ^1H NMR (200 MHz, DMSO-d_6): δ_H 9.72 (d, 2H), 9.11 (t, 1H). ^{13}C NMR (100 MHz, DMSO-d_6): δ_C 149.64, 144.23, 127.13. MS (EI, 70 eV) (*m*/*z*, %): 169 (63) [M^+], 123 (76), 93 (10), 77 (29), 76 (47), 66 (28), 50 (100), 30 (46).

Matrix Isolation Spectroscopy. Matrix isolation experiments were performed by standard techniques[50] with an APD DE-204SL and an APD DE-202 Displex closed cycle helium cryostat. Matrices were produced by codeposition of the compound with a large excess of argon (Messer Griesheim, 99.9999%) on top of a cold CsI window with a rate of approximately 0.15 mmol/min. To obtain optically clear matrices, the spectroscopic window was retained at 30 K during deposition and subsequently cooled to 10 K. FVP experiments were carried out without additional heating of the spectroscopic window (temperature around 15 K). Matrix infrared spectra were recorded with Bruker IFS 66 and Equinox 55 FTIR spectrometers with a standard resolution of 0.5 cm^{-1} using a N_2(l) cooled MCT detector in the range 400−4000 cm^{-1}. Irradiation at 254 nm was carried out with a Gräntzel low-pressure mercury arc lamp.

Computational Methods. Geometries of all species were fully optimized at the BLYP level[51,52] (in some cases, the B3LYP,[52,53] BPW91,[51,54] and B3PW91[53,54] functionals have been used for comparison), and analytic second derivatives were calculated to characterize stationary points as minima or transition states. Tight convergence criteria for gradients (with maximum residual forces on nuclei below 0.000015 au) and a full (99, 590) integration grid, having 99 radial shells per atom and 590 angular points per shell, have been used throughout to obtain accurate values for geometries and low-frequency vibrational modes. A spin-unrestricted formalism has been used generally, where for calculations on singlet states the initial guess frontier orbitals have been mixed to destroy (spin-)symmetry and in each step during a geometry optimization or IRC calculation a new initial guess was calculated. Whenever a spin-restricted solution was obtained, it was further tested for instabilities by calculating the eigenvalues of the Hermitian stability matrices.[55] For general considerations regarding DFT calculations on biradicals, see ref 56 and literature cited therein. For many transition states localized in this work, the corresponding IRCs were calculated in mass-weighted coordinates with a step size of 0.05 $amu^{1/2}$ bohr.[45] All DFT calculations were carried out with Gaussian 98.[57]

Single-point energy computations utilized the Molpro 2000.1 program package employing different levels of theory.[58] Because of the well-known instability problems associated with coupled-cluster calculations including all single, double, and perturbatively estimated triple excitations [CCSD(T)] for systems with significant multireference character, BCCD(T) calculations have routinely been carried out for comparison.[59] Brueckner orbitals eliminate contributions from single excitations in the coupled-cluster ansatz, which often (but not always)[59d] cures the shortcomings of the singlereference CCSD(T) approach [a good example is the energy of (*Z*)-**35**, cf. Table 6]. In several cases, these computations were complemented by multireference methods all of which are based on complete active space self-consistent field (CASSCF) wave functions. For benzynes (and related C_6H_4 isomers), the eight electron/eight orbital active space covers the six benzene valence π orbitals and the two formally nonbonding σ orbitals at the dehydrocarbons. For the pyridynes (C_5H_3N), this space was extended by the nitrogen lone pair, resulting in a CASSCF(10,9) wave function. Dynamic electron correlation was covered by perturbation theory to second- (CAS-RS2) or third-order (CAS-RS3)[60] or by internally contracted configuration interaction including single and double excitations (CAS-CISD).[61] If not mentioned otherwise, MR-CI energies refer to Davidson-corrected[62] values (CAS-CISD+Q). In post-(CAS)SCF calculations, the core orbitals were kept frozen.

For most computations, Dunning's correlation consistent cc-pVTZ basis set with (10s5p2d1f)[4s3p2d1f] contraction for C and N and (5s2p1d)[3s2p1d] contraction for H was used.[63] In selected cases, we also employed cc-pVDZ and cc-pVQZ basis sets to study the convergence behavior.[64] Vibrational spectra of iodine-containing molecules had to be calculated with the 6-311G(d,p) Pople type basis set, as no correlation consistent basis sets are available for I.[65]

Electron densities for AIM (atoms in molecules) analysis[40] have been recalculated using Cartesian d and f functions (7d, 10f), whereas pure angular momentum functions are used for all geometry optimizations and single-point energy calculations. The AIM 2000 program was used

(49) Plazek, E. *Rec. Trav. Chim.* **1953**, *72*, 569.
(50) Dunkin, I. R. *Matrix-Isolation Techniques*; Oxford University Press: Oxford, 1998.
(51) Becke, A. D. *Phys. Rev. A* **1988**, *38*, 3098.
(52) Lee, C.; Yang, W.; Parr, R. G. *Phys. Rev. B* **1988**, *37*, 785.
(53) (a) Becke, A. D. *J. Chem. Phys.* **1993**, *98*, 5648. Compare (b) Stevens, P. J.; Devlin, F. J.; Chablowski, C. F.; Frisch, M. J. *J. Phys. Chem.* **1994**, *98*, 11623.
(54) Perdew, J. P.; Burke, K.; Wang, Y. *Phys. Rev. B* **1996**, *54*, 16533.
(55) Bauernschmitt, R.; Ahlrichs, R. *J. Chem. Phys.* **1996**, *104*, 9047.
(56) (a) Cremer, D.; Filatov, M.; Polo, V.; Kraka, E.; Shaik, S. *Int. J. Mol. Sci.* **2002**, *3*, 604. (b) Gräfenstein, J.; Kraka, E.; Filatov, M.; Cremer, D. *Int. J. Mol. Sci.* **2002**, *360*. (c) Polo, V.; Kraka, E.; Cremer, D. *Theor. Chem. Acc.* **2002**, *107*, 291. (d) Polo, V.; Kraka, E.; Cremer, D. *Mol. Phys.* **2002**, *100*, 1771. (e) Gräfenstein, J.; Hjerpe, A. M.; Kraka, E.; Cremer, D. *J. Phys. Chem. A* **2000**, *104*, 1748.
(57) Frisch, M. J.; Trucks, G. W.; Schlegel, H. B.; Scuseria, G. E.; Robb, M. A.; Cheeseman, J. R.; Zakrzewski, V. G.; Montgomery, J. A., Jr.; Stratmann, R. E.; Burant, J. C.; Dapprich, S.; Millam, J. M.; Daniels, A. D.; Kudin, K. N.; Strain, M. C.; Farkas, O.; Tomasi, J.; Barone, V.; Cossi, M.; Cammi, R.; Mennucci, B.; Pomelli, C.; Adamo, C.; Clifford, S.; Ochterski, J.; Petersson, G. A.; Ayala, P. Y.; Cui, Q.; Morokuma, K.; Malick, D. K.; Rabuck, A. D.; Raghavachari, K.; Foresman, J. B.; Cioslowski, J.; Ortiz, J. V.; Stefanov, B. B.; Liu, G.; Liashenko, A.; Piskorz, P.; Komaromi, I.; Gomperts, R.; Martin, R. L.; Fox, D. J.; Keith, T.; Al-Laham, M. A.; Peng, C. Y.; Nanayakkara, A.; Gonzalez, C.; Challacombe, M.; Gill, P. M. W.; Johnson, B.; Chen, W.; Wong, M. W.; Andres, J. L.; Gonzalez, C.; Head-Gordon, M.; Replogle, E. S.; Pople, J. A. *Gaussian 98*; Gaussian, Inc.: Pittsburgh, PA, 1998.
(58) Werner, H.-J.; Knowles, P. J. *Molpro 2000.1*; Birmingham, 1999.
(59) (a) Lee, T. J.; Scuseria, G. E. In *Quantum Mechanical Electronic Structure Calculations with Chemical Accuracy*; Langhoff, S. R., Ed.; Kluwer Academic Publishers: Dordrecht, 1997. (b) Bartlett, R. J. In *Modern Electronic Structure Theory*; Yarkony, D. R., Ed.; World Scientific: Singapore, 1995. (c) Taylor, P. R. In *Lecture Notes in Quantum Chemistry*; Roos, B. O., Ed.; Springer: Berlin, 1994. See also (d) Crawford, T. D.; Stanton, J. F. *J. Chem. Phys.* **2000**, *112*, 7873 and references therein.
(60) Werner, H.-J. *Mol. Phys.* **1996**, *89*, 645.
(61) (a) Werner, H.-J.; Knowles, P. J. *J. Chem. Phys.* **1988**, *89*, 5803. (b) Knowles, P. J.; Werner, H.-J. *Chem. Phys. Lett.* **1988**, *145*, 514.
(62) (a) Duch, W.; Diercksen, G. H. F. *J. Chem. Phys.* **1994**, *101*, 3018. (b) Langhoff, S. R.; Davidson, E. R. *Int. J. Quantum Chem.* **1974**, *8*, 61.
(63) (a) Woon, D. E.; Dunning, T. H. *J. Chem. Phys.* **1993**, *98*, 1358. (b) Kendall, R. A.; Dunning, T. H.; Harrison, R. J. *J. Chem. Phys.* **1992**, *96*, 6796. (c) Dunning, T. H. *J. Chem. Phys.* **1989**, *90*, 1007.
(64) (a) Dunning, J. H., Jr. *J. Phys. Chem. A* **2000**, *104*, 9062. (b) Dunning, J. H., Jr.; Peterson, K. A. *J. Chem. Phys.* **2000**, *113*, 7799. (c) Petersson, G. A.; Frisch, M. J. *J. Phys. Chem. A* **2000**, *104*, 2183.
(65) (a) Glukhovstev, M. N.; Pross, A.; McGrath, M. P.; Radom, L. *J. Chem. Phys.* **1995**, *103*, 1878. (b) Basis sets were obtained from the Extensible Computational Chemistry Environment Basis Set Database, Version 6/19/03, as developed and distributed by the Molecular Science Computing Facility, Environmental and Molecular Sciences Laboratory, which is part of the Pacific Northwest Laboratory, P.O. Box 999, Richland, WA 99352, and funded by the U.S. Department of Energy. The Pacific Northwest Laboratory is a multiprogram laboratory operated by Battelle Memorial Institute for the U.S. Department of Energy under contract DE-AC06-76RLO 1830. Contact David Feller or Karen Schuchardt for further information.
(66) Biegler-König, F.; Schönbohm, J.; Bayles, D. *J. Comput. Chem.* **2001**, *22*, 545.
(67) (a) Wolinski, K.; Hilton, J. F.; Pulay, P. *J. Am. Chem. Soc.* **1990**, *112*, 8251. (b) Ditchfield, R. *Mol. Phys.* **1974**, *27*, 789.

for topological electron density analysis.[66] Chemical shifts were calculated at the BLYP level by the gauge-independent atomic orbital (GIAO) method.[67]

Acknowledgment. In memoriam Paul Heimbach (1934−1991). This work was financially supported by the Deutsche Forschungsgemeinschaft and the Fonds der Chemischen Industrie. We thank Dr. H. F. Bettinger for stimulating discussions.

Supporting Information Available: Energies and geometries (Cartesian coordinates) for all minima and transition states, structures along several IRCs, and additional spectroscopic details. This material is available free of charge via the Internet at http://pubs.acs.org.

JA039142U